Technische Universität München

Analytical and Numerical Approaches for the Computation of Aeroelastic Sensitivities Using the Direct and Adjoint Methods

Lukas Scheucher, B.Sc.

Master Thesis

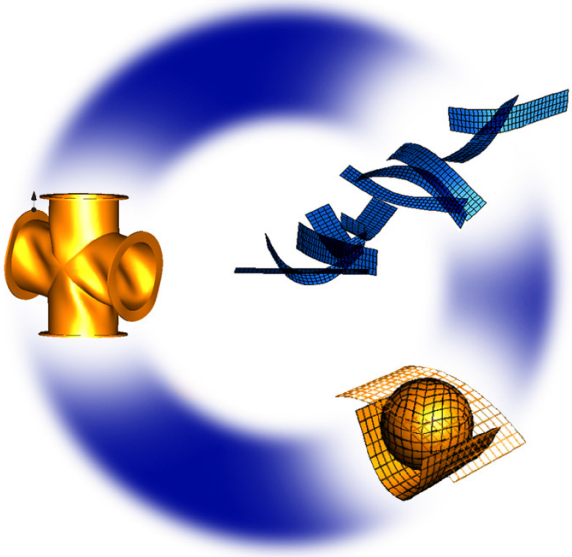

SUPERVISOR:
Dr.-Ing. Alexander Popp, Dr.-Ing. Georg Hammerl
popp@lnm.mw.tum.de

Institute for Computational Mechanics
Prof. Dr.–Ing. W. A. Wall
Technische Universität München
Boltzmannstraße 15
85748 Garching b. München (Germany)

Own work declaration

Hereby I confirm that this is my own work and I referenced all sources and auxiliary means used and acknowledged any help that I have received from others as appropriate.

(location, date) (signature)

Abstract

This is the most often read section. It will determine if someone actually bothers to read more of what you've written. Only write this section after you have completed your report. The abstract consist of only one paragraph, mostly limited to 200-300 words. Literally, a summary of your work. Write a sentence or two about each of the main sections of your report, as discussed in this section. When summarizing results, make the reader aware of the most important results (including numbers when applicable) and important conclusions or questions that follow from these.

Zusammenfassung

german version of your abstract.

Contents

List of Figures

Nomenclature

Operators

Algebraic operations

A^T	Transpose of a tensor	`T`
A^{-1}	Inverse of a tensor	`inv`
$\bar{a}$	Average component of a quantity	`av`
a'	Fluctuating component of a qunatity	`fluc`
$\|a\|$	Norm of a quatntity	`norm`

Analytic operations

$\ddot{A}$	Second time derivative at a fixed refrence position	`dderivtime`
$\dot{A}$	First time derivative at a fixed reference position	`derivtime`
$\frac{\partial A}{\partial B}$	partial derivative of one argument with respect to the other	`pdfrac`
$\frac{\partial^2 A}{\partial B^2}$	Second partial derivative of one argument with respect to the other	`ppdfrac`
$\frac{DA}{DB}$	Material time derivative	`mfrac`
$\frac{\mathrm{d}A}{\mathrm{d}B}$	First total derivative of one argument with respect to the other	`tfrac`

Representation of scalars, tensors and other quantities

a	Scalar quantity	`s`
$\boldsymbol{a}$	Vector quantity	`v`
$\boldsymbol{A}$	Matrix quantity	`m`
A, a	continous quantity	`c`
A, a	discrete quantity	`d`
$a^{(k)}$	Iteration index in the optimization loop	`it`
$a^{(k)}$	Iteration index in the optimization loop	`ito`
$a^{(n)}$	Iteration index in thestaggered algorithm	`its`
$\bar{A}$	Fictious entity	`fic`
$\mathcal{O}(A)$	Order of magnitude	`order`

Symbols

3-field formulations

$\mathbf{T}_p$	Interface projection matrix from fluid to structure mesh	`ifaceprojFt`
$\boldsymbol{H}_2$	Second order Jacobian	`jactwo`
$\mathbf{S}$	Turbulence term	`turbmat`
$\mathbf{T}_u$	Interface projection matrix from structure to fluid mesh	`ifaceprojSt`
$\mathbf{F}$	Convective part of the flux matrix	`fluxmatconv`
$\mathbf{w}$	Discrete fsluid state vector	`dfstate`
$\mathcal{D}_{gov}$	State equation of the mesh	`EOSmesh`
$\boldsymbol{P}$	Fluid load TODO	`load`
$\boldsymbol{a_u}$	Adjoint structure displacement	`structdispa`
$\boldsymbol{w}$	Fluid state vector	`fstate`
$\boldsymbol{P}_F$	Fluid load	`fload`
$\mathcal{S}_{gov}$	State equation of the structure	`EOSstruct`
$\boldsymbol{a_w}$	Adjoint fluid state vector	`fstatead`
$\tilde{\boldsymbol{w}}$	Primitive ffluid state vector	`fstateprim`
$\dot{\boldsymbol{x}}$	Fluid mesh motion	`mms`
$\mathbf{G}$	diffusive part of the flux matrix	`fluxmatdiff`
$\mathcal{F}_{gov}$	State equation of the fluid	`EOSfluid`
S	Source term in the Reynolds Averaged Navier-Stokes (RANS) equations	`turbulences`
$\boldsymbol{a_x}$	Adjoint fluid mesh motion	`mmsad`
$\boldsymbol{w}_{RANS}$	Augumentes fluid state vector in the RANS formulation	`fstaterans`
$\boldsymbol{P}_T$	Structure load	`sload`
$\boldsymbol{u}$	Structure displacement	`structdisp`
$\mathbf{A}$	Diagonal matrix with vell volumes	`cellvolmat`
$\boldsymbol{\chi}$	Additional fluid state variable introduced by the turbulence model	`turbparamve`

Fluid Structure Interaction

$\mathcal{P}$	State equation of the structure	`strucstateq`
$\mathcal{D}$	State equation of the mesh motion	`mmsstateeq`
$\mathcal{F}$	State equation of the fluid	`fluidstateq`

Sturctural Analysis

$\mathbf{K}$	FE stiffness matrix	`stiffmat`
u	Displacement vector	`disp`
$\mathbf{d}$	Interface displacement	`ifacedispvec`
$\mathbf{u}$	Discrete displacement vector	`dispvec`
$\boldsymbol{x}$	Mesh motion	`motion`

Optimization

s	Abstract optimazation variable	`absvar`
q	Optimization criterium	`optcrit`
ϵ^{SA}	Specified tolerance in the Sensitivity analysis	`tolsa`
$\boldsymbol{\eta}$	Lagrange multipliers of the equality constraints	`lagmultseq`
L	Lagrangian function of the optimization problem	`Lagfunc`
$\boldsymbol{s}$	Vector of abstract optimization variables	`absvars`
$\boldsymbol{g}$	Non-equality constraints	`neqctr`
$\boldsymbol{\gamma}$	Lagrange multipliers of the inequality constraints	`lagmultsneq`
$\boldsymbol{q}$	Vector of optimization criteria	`optcrits`
$\boldsymbol{d}$	Physical design parameters	`physvars`
z	Target cost function	`costfunc`
$n_{\boldsymbol{g}}$	Number of non-equality constraints	`numneqctr`
$\boldsymbol{h}$	Equality constraints	`eqctr`
$\boldsymbol{a}$	Adjoint solutions	`adjoints`
$n_{\boldsymbol{h}}$	Number of equality constraints	`numeqctr`

Fluid Mechanics

p	Pressure	`pres`
$\mathcal{F}$	Convective fluxes	`fluxesconv`
$\boldsymbol{P}$	Matrix that contains the eigenvectors of the jacobian matrix of $\mathbf{F}$	`jaceigvecs`
T	Fluid temperature	`temp`
v_3	Fluid velocity in z-direction	`fluidvelz`
$\boldsymbol{\Lambda}$	Diagonal matrix that contains the eigenvalues of the jacobian matrix of $\mathbf{F}$	`jaceigvals`
$\mathcal{H}$	Jacoian matrix	`jac`
ρ	Density	`dens`
μ	Dynamic viscosity	`viscosdyn`
$\mathbf{I}$	Identity matrix	`eye`
ν	Kinematic viscosity	`viscoskin`
$\mathcal{A}$	Flux Jacobian	`fluxjac`
τ	Deviatoric fluid stress tensor	`fluidstresscc`
$\mathcal{G}$	Diffusive fluxes	`fluxesdiff`
q	Heat flux comopnenent	`heatfluxcomp`
k	Thermal conductivity of the fluid	`thermcond`
E	Total energies	`energytot`
R_e	Reynolds number	`reynolds`
$\boldsymbol{q}$	Heat flux vector	`heatflux`
γ	Specific heat ratio	`specheatratic`
v_2	Fluid velocity in y-direction	`fluidvely`
e	Internal energy	`energyint`
v	Fluid velocity vector	`fluidvelcomp`
v_1	Fluid velocity in x-direction	`fluidvelx`
$\boldsymbol{M}$	Averaging function associated with the Roe flux	`roeavgfunc`

Abbrevations

SQP Sequential Quadratic Programming

GSE Global Sensitivity Equations

SA Sensitivity Analysis

VOF Volume of Fluid Method

GFM Ghost Fluid Method

GFMP Ghost Fluid Method of the Poor

EOS Equation of State

JWL Jones-Wilkins-Lee

PG Perfect Gas

SG Stiffened Gas

MUSCL Monotonic Upwind scheme for Conservation Laws

FIVER Finite Volume Method with exact two-phase Riemann Integrals

RANS Reynolds Averaged Navier-Stokes

FV Finite Volumes

FD Finite Differences

FE Finite Elements

SA Sensitivity Analysis

LNM Lehrstuhl für Numerische Mechanik(Institute for Computational Mechanics)

TUM Technical University of Munich

CFD Computational Fluid Dynamics

ALE Arbitrary Lagrangian Eulerian

VOF Volume of Fluid Methods

DFP Davidon-Fletcher Powell formula

BFGS Broyden-Fletcher-Goldfarb-Shanno algorithm

LDR Lift over Drag Ratio

NSE Navier Stokes Equations

NSME Momentum Equation of the Navier Stokes Equations

NSCE Continuity Equation of the Navier Stokes Equations

NSEE Energy Equation of the Navier Stokes Equations

PDE Partial Differential Equation

CG Conjugate Gradient

PCG Preconditioned Conjugate Gradient

SA Sensitivity Analysis

CFD Computational Fluid Dynamics

FSI Fluid Structure Interaction

FRG Farhat Research Group

1 About this template

The purpose of this document is two-fold:
Firstly, this is a plain and simple template with the most basic LaTeX-commands and structures introduced that are needed for writing a thesis in LaTeX. It should be sufficient for 95% of the theses submitted at LNM - this means that completeness is not claimed. It is recommended to stick to these basic suggestions, knowing that other - possibly better - philosophies or styles exist. In case a more complex structure is needed, refer to literature or the web, although you should think twice about introducing a much more complex structure.
Secondly, this report gives some basic suggestions on what the structure of the report should look like and also some brief description about typically expected content.

Figure 1: aaa bbb

Please note:

- Significant changes to the document style, layout and structure should only be done according to prior agreement with your supervisor.
- compile the template with the following command
  `latex LaTeX_template_v04.tex && dvipdfm LaTeX_template_v04.dvi`
- if you encounter problems with dvipdfm, you can also use
  `latex LaTeX_template_v04.tex && dvi2ps LaTeX_template_v04.dvi && ps2pdf LaTeX_template_v04.ps`
- if you use texmaker, or a similar LaTeX editor, declare `LaTeX_template_v04.tex` as master document
- the latex compiler might requires 2 or 3 runs, until newly created references are resolved correctly
- the bibtex file has to be compiled seperately

2 Fluid mechanics

2.1 Eulerian and Lagrangian view

In time dependent analytical physics there are two basic concepts of how to view a system of interest: the Eulerian and the Lagrangian approach. It shall be stressed here, that Eulerian view and Euler equations are two totally separate things.
One view this issue from different perspectives, but what the difference boils down to is the interpretation of the time derivative. Since we will be using the different derivatives frequently in this thesis, a short introduction shall be provided.

2.1.1 Material derivative

The material derivative of a property, is a derivative(rate of change), that follows a specific particle 'p'. That means that at every time instance the material derivative gives as the current value of the property of a specific particle. Since in general, a particle will move its position in time quite a lot, some mean is required to track the particles motion. The material derivative is also known as the Lagrangian concept, and is commonly used in Solid mechanics, since the motion of the solid particles is typically little, or at least nearly uniform over the body, which makes position tracking easy.

2.1.2 Eulerian derivative

The Eulerian derivative takes a different approach. It refers to a fixed frame of reference in the domain, and gives the rate of change at that specific position. Due to the particle movement, it typically refers to different particles at different times. Material and Eulerian derivatives can be linked via the so-called convective rate of change as:

$$\underbrace{\frac{D\boldsymbol{G}}{Dt}}_{\text{Lagrangian rate of change}} = \underbrace{\frac{\partial \boldsymbol{G}}{\partial t}}_{\text{Eulerian rate of change}} + \underbrace{\boldsymbol{v} \cdot \nabla \boldsymbol{G}}_{\text{Convective rate of change}} \tag{1}$$

In fluid mechanics the Eulerian concept is typically prefered.
However, when looking at fluid-structure interaction problems, the interface is typically moving. To account for that motion in the fluid, one either has to come up with some cell-intersection approach, or the fluid-mesh has to be deformed to.
An appealing and straightforward approach to do so, is the so called Arbitrary Lagrangian Eulerian(Arbitrary Lagrangian Eulerian (ALE)) approach. As the name suggest, it is a hybrid between Eulerian and Lagrangian point of view. The ALE approach allows to utilize the best of both approaches. The mesh can either be fixed, moved with the continuum in an Eulerian manner, or be moved in some arbitrarily specified manner inbetween. The ALE method can handle larger distortions than a pure Eulerian would, while still allowing to keep interface continuity between the structure and the fluid, such that no intersection of fluid cells is necessary.

In this thesis, both Eulerian and ALE methods will be covered. In general, no recommendation on to prefer one or the other method can be given. Instead, one should always be aware of the pros and cons of either method and choose the appropriate one for a specific problem accordingly.

2.2 Basic equations of fluid mechanics

The physics of fluid motion are governed by the so-called Navier Stokes Equations (NSE). These equations were derived independently of one another by Claude-Louis Navier and George Gabriel Stokes as a generalization of the Euler-equations that now includes viscosity effects. In general one distinguishes the incompressible and the compressible NSE. The validity of their application depends on the problem setup. As a rule of thumb, flows with Mach-numbers lower than 0.3 can usually be safely approximated by the incompressible NSE.
The Navier stokes equation consist of the Momentum Equation of the Navier Stokes Equations (NSME), the Continuity Equation of the Navier Stokes Equations (NSCE) and, if the compressible equations are solved, the Energy Equation of the Navier Stokes Equations (NSEE). In the literature, the term NSE is often synonymously used for the NSCE, in this thesis however, with NSE we will always refer to the full set of equations and will explicitly name the momentum, continuity or energy equation otherwise.

2.2.1 Incompressible Navier Stokes Equations

The incompressible NSE are derived by putting a few assumptions on the Cauchy stress tensor:

- Galilean invariance of the fluid stress tensor
- Isotropy of the fluid
- The stokes stress constitutive equation applies: $\boldsymbol{\tau} = 2\mu\boldsymbol{\epsilon}$ with $\boldsymbol{\epsilon} = \frac{1}{2}(\nabla\boldsymbol{v} + (\nabla\boldsymbol{v})^T)$

In convective form, the incompressible NSME can be written as

$$\overbrace{\underbrace{\frac{\partial \boldsymbol{v}}{\partial t}}_{\text{Variation}} + \underbrace{(\boldsymbol{v}\cdot\nabla)\boldsymbol{v}}_{\text{Convection}}}^{\text{Inertia per volume}} - \overbrace{\underbrace{\nu\nabla^2\boldsymbol{v}}_{\text{Diffusion}} = -\underbrace{\nabla\boldsymbol{w}}_{\text{Internal source}}}^{\text{Divergence of stress}} + \underbrace{g}_{\text{External source}} \tag{2}$$

where $\boldsymbol{w}$ is the specific thermodynamic work, which satisfies

$$\nabla\boldsymbol{w} = \frac{1}{\rho}\nabla p \tag{3}$$

And the incompressible NSCE can be written as

$$\nabla\cdot\boldsymbol{v} = 0 \tag{4}$$

It shall be noted, that in the incompressible NSE, the pressure can only be solved up to a certain constant. The pressure at a certain point therefore has to be fixed, or the system will be singular.

2.2.2 Compressible Navier Stokes Equations

Compared to the incompressible NSE, the compressible NSE introduce one additional unknown, since the density can now vary. To close the system, one additional equation is required: the energy equation.
The compressible NSE are derived by making the following assumptions:

- Galilean invariance of the stress tensor
- Linearity of the stress in the velocity gradient: $\boldsymbol{\tau}(\nabla \boldsymbol{v}) = \boldsymbol{C} : (\nabla \boldsymbol{v})$, where $\boldsymbol{C}$ is called the viscosity or elasticity tensor.
- Isotopy of the fluid

The compressible NSME can be written as

$$\frac{\partial \boldsymbol{v}}{\partial t} + \boldsymbol{v} \cdot \nabla \boldsymbol{v} = -\frac{\partial 1}{\partial \rho} \nabla p + \nu \nabla^2 \boldsymbol{v} + \frac{1}{3} \nu \nabla (\nabla \cdot \boldsymbol{v}) + g \tag{5}$$

eq:nsg_compressible

where it shall be noted that for the special case of an incompressible flow, the volume of the fluid elements is constant, resulting in a solenoidal velocity field. Thus $\nabla \cdot \boldsymbol{v} = \boldsymbol{0}$ and $\nabla p = 0$, which gives equation 2.
The NSCE now takes into accounts for the variable density

$$\frac{\partial \rho}{\partial t} = \nabla \cdot (\rho \boldsymbol{v}) = 0 \tag{6}$$

And finally the NSEE writes

$$\frac{\partial s}{\partial t} = -\boldsymbol{v} \cdot s + \frac{Q}{T} \tag{7}$$

where s is the entropy per unit mass, Q is the heat transferred, and T is the temperature.

2.2.3 Euler equations

The Euler equations can be regarded as a special case of the Navies stokes equations where the diffusive(viscous) contributions are neglected. Dimension analysis [1] reveals that this is usually justified for high Mach numbers and distant from walls. In fact, boundary Layer theory suggests that a lot of problems can be well approximated by solving the full, diffusive equations only near the wall boundary and using the Euler equations everywhere else. Although the Euler equations can be derived for both incompressible and compressible flows, the statement above suggests that only the compressible ones give actual, physically correct results. We therefore restrict

our considerations to the compressible Euler equations.
Summing up, these equations can be written in convective form as

$$\begin{cases} \frac{\partial \rho}{\partial t} + \boldsymbol{v} \cdot \nabla \rho + \rho \nabla \cdot \boldsymbol{v} = 0 & \text{Continuity equation} \\ \frac{\partial \boldsymbol{v}}{\partial t} + \boldsymbol{v} \cdot \nabla \boldsymbol{v} + \frac{p}{\rho} = \boldsymbol{g} & \text{Momentum equation} \\ \frac{\partial e}{\partial t} + \boldsymbol{v} \cdot \nabla e + \frac{p}{\rho} \nabla \cdot \boldsymbol{v} = 0 & \text{Energy equation} \end{cases} \tag{8}$$

2.2.4 Conservative Form

For the purpose of FV discretization one usually brings the equations into the so-called conservative form, which can be written generally as

$$\frac{\mathrm{d}\boldsymbol{\xi}}{\mathrm{d}t} + \nabla \cdot f(\boldsymbol{\xi}) = \mathbf{0} \tag{9}$$ eq:conservative_form_general

(10)

where $\boldsymbol{\xi}$ is the conserved qunatity of interest and $f(\boldsymbol{\xi})$ is denoted as "flux function". This equation can then be transformed into an integral form using the divergence theorem

$$\frac{\mathrm{d}}{\mathrm{d}t} \int_V \boldsymbol{\xi} dV + \int_{\partial V} f(\boldsymbol{\xi}) \cdot \boldsymbol{n} dS \tag{11}$$ eq:conservation_form_integral

This equations states that the rate of change of the integral of the quantity $\boldsymbol{\xi}$ over an arbitrary control volume V is equal to the negative of the "flux" through the boundary of the control volume ∂V.
A simple choice for f would be $f(\xi) = \xi \boldsymbol{v}$, which means that the quantity $\boldsymbol{\xi}$ follows the fluid field and gives the so-called "advection equation".
Although one form is derived from the other, these two are not equivalent. Particularly, it is possible to find solutions to the integral equations that are non-differentiable and therefore not a solutions to the differential form. This leads to so called "weak solutions" and is the cause for many numerical difficulties in the finite volume simulation of such problems.

This thesis focuses on the compressible NSE only. They can be brought to conservative form as:

$$\frac{\partial \boldsymbol{w}}{\partial t} + \nabla \cdot \mathcal{F}(\boldsymbol{w}) + \nabla \cdot \mathcal{G}(\boldsymbol{w}) = \mathbf{0} \tag{12}$$ eq:nsg_conservative_form

where, comparing to the general conservative form, one can see that $\boldsymbol{\xi} = \boldsymbol{w}$ and $f(\boldsymbol{\xi}) = \mathcal{F}(\boldsymbol{w}) + \mathcal{G}(\boldsymbol{w})$
In the conservative form of the NSE the so-called "fluid state vector" $\boldsymbol{w}$ is defined as

$$\boldsymbol{w} = \begin{bmatrix} \rho \\ \rho \boldsymbol{v} \\ E \end{bmatrix} \tag{13}$$ eq:fstate_definition

with

$$\boldsymbol{v} = \begin{bmatrix} v_1 \\ v_2 \\ v_3 \end{bmatrix} \tag{14}$$ eq:fluidvel_definition

denoting the fluid velocity vector.

The total energy E can be computed as a sum of the so called internal energy and the kinematic energy due to fluid velocity as

$$\underbrace{E}_{\text{total energy}} = \underbrace{\rho e}_{\text{internal energy}} + \underbrace{\frac{1}{2}\boldsymbol{v}^T\boldsymbol{v}}_{\text{kinematic energy}} \tag{15}$$ eq:energytot

Bringing the convective form of the compressible NSE (5) into the conservative form (12), one can derive the convective fluxes $\mathcal{F}$ as

$$\mathcal{F} = \boldsymbol{w}\boldsymbol{v}^T + p \begin{bmatrix} 0 \\ \mathbf{I} \\ \boldsymbol{v}^T \end{bmatrix} \tag{16}$$ eq:fluxesconv

$$= \begin{bmatrix} \rho\boldsymbol{v}^T \\ \rho(\boldsymbol{v}\boldsymbol{v}^T) + p\mathbf{I} \\ (E+p)\boldsymbol{v}^T \end{bmatrix} \tag{17}$$

$$= \begin{bmatrix} \rho v_1 & \rho v_2 & \rho v_3 \\ p + \rho {v_1}^2 & \rho v_1 v_2 & \rho v_1 v_3 \\ \rho v_2 v_1 & p + \rho {v_2}^2 & \rho v_2 v_3 \\ \rho v_3 v_1 & \rho v_3 v_2 & p + \rho {v_3}^2 \\ v_1(E+p) & v_1(E+p) & v_1(E+p) \end{bmatrix} \tag{18}$$

depending on the algorithm, one or another form can be advantageous.

The diffusive fluxes can be written as

$$\mathcal{G} = \begin{bmatrix} \mathbf{0} \\ \boldsymbol{\tau} \\ \boldsymbol{\tau}\boldsymbol{v} + \boldsymbol{q} \end{bmatrix} \tag{19}$$ eq:fluxes_diff

$$= \begin{bmatrix} 0 & 0 & 0 \\ -\tau_{xx} & -\tau_{yx} & -\tau_{zx} \\ -\tau_{xy} & -\tau_{yy} & -\tau_{zy} \\ -\tau_{xz} & -\tau_{yz} & -\tau_{zz} \\ -q_x - v_1\tau_{xx} - v_1\tau_{yx} - v_1\tau_{zx} & -q_y - v_1\tau_{xy} - v_1\tau_{yy} - v_1\tau_{zy} & -q_z - v_1\tau_{xz} - v_1\tau_{yz} - v_1\tau_{zz} \end{bmatrix}^T \tag{20}$$

The definition of the stress tensor depends of the fluid model used. For the simple case of a Newtonian fluid, it can be written as

$$\boldsymbol{\tau} = \mu(\nabla\boldsymbol{v} + (\nabla\boldsymbol{v})^T) + \lambda(\nabla\cdot\boldsymbol{v})\mathbf{I} \tag{21}$$ eq:fluidstress

For the relation between Temperature and heat flux an assumption has to be made. Most often, a simple Fourier's law is assumed

$$\boldsymbol{q} = -k\nabla T \tag{22}$$ eq:heatflux

2.2.5 Euler equations

The euler equations are a simplified form of the Navier-Stokes Equations (2)(5), where the viscous effects are neglected by setting $\mathcal{G} = \mathbf{0}$.

$$\frac{\partial \boldsymbol{w}}{\partial t} + \nabla \cdot \mathcal{F}(\boldsymbol{w}) = \mathbf{0} \tag{23}$$ eq:euler

The Euler equations are appropriate for a wide range of applications. A typical indicator is the Reynolds number, which describes the ratio between inertial forces and viscous forces:

$$R_e = \frac{\rho \boldsymbol{v} L}{\mu} = \frac{\boldsymbol{v} L}{\nu} \tag{24}$$ eq:reynolds

where L describes a characteristic length.

A high Reynolds number thus indicates that the flow is dominated by inertial forces, thus the Euler Equations should give satisfying results. However, an Euler flow lacks the ability to represent stick wall boundary conditions, thus it is unable to represent boundary layers.

2.2.6 Equations of State

Looking at the above Equations, one might notice that the number of unknowns is greater than the number of equations. Particularly, the pressure only appears in Equation (16) and is not linked to the other formulas. This problem is solved by introducing an Equation of State (EOS) that relates pressure, internal energy and density. The EOS depends on the fluid model, some well-known ones are: Perfect Gas (PG), Stiffened Gas (SG), Jones-Wilkins-Lee (JWL).
For the simplest one, PG, the EOS can be written as

$$p = (\gamma - 1)\rho e \tag{25}$$ eq:eos_pg

2.2.7 Reynolds Averaged Navier-Stokes Equations

The Reynolds Averaged Navier-Stokes (RANS) Equations are time-averaged equations of motion for the fluid.

$$\boldsymbol{w} \to \bar{\boldsymbol{w}} = \lim_{T\to\infty} \frac{1}{T} \int_{t^0}^{t^0+T} \boldsymbol{w} dt \tag{26}$$ eq:rans_averaging

The main idea of the approach is to decompose an instantaneous quantity into time-averaged and fluctuating components

$$\boldsymbol{w} = \underbrace{\bar{\boldsymbol{w}}}_{time-average} + \underbrace{\boldsymbol{w}'}_{fluctuation} \tag{27}$$ eq:rans_decomposition

When substituting this decomposition back into the NSE(and injecting several other approximations), a closure problem induced by the arising non-linear Reynolds stress term $R_{eij} = -v_i{}'\bar{v}_j{}'$ arises. Additional modeling is therefore required to close the RANS equations, which has led to many different turbulence models.

Whatever turbulence model is chosen, the fluid-state vector is augmented by the m parameters of the turbulence model

$$\boldsymbol{w}_{RANS} \leftarrow \begin{bmatrix} \boldsymbol{w} \\ \chi_1 \\ \vdots \\ \chi_m \end{bmatrix} = \begin{bmatrix} \rho \\ \rho \boldsymbol{v}^T \\ E \\ \chi_1 \\ \vdots \\ \chi_m \end{bmatrix} \tag{28}$$

The RANS equations can then be written as

$$\frac{\partial \bar{\boldsymbol{w}}}{\partial t} + \nabla \cdot \mathcal{F}(\bar{\boldsymbol{w}}) + \nabla \cdot \mathcal{G}(\bar{\boldsymbol{w}}) = \mathsf{S}(\bar{\boldsymbol{w}}, \chi_1, \cdots, \chi_m) \tag{29}$$ eq:rans_eqautions

3 The Finite Volume method

3.1 General

Like Finite Differences (FD) or Finite Elements (FE), the Finite Volumes (FV) method is a mean of solving a Partial Differential Equation (PDE) by transforming it into a discrete algebraic form. In the field of fluid mechanics, the finite volume method is the most popular approach. Other than FD or FE, the finite volume is conservative by construction. In contrast to FD it can easily be implemented for unstructured grids. Compared to the FE method, where boundary conditions come naturally from the formulation, this causes some difficulties in FV.
It shall also be mentioned that the introduction of stabilization schemes(like streamline upwinding), is much easier in an FV formulation. Overall, for Computational Fluid Dynamics (CFD), FV has so far shown to be the best compromise between accuracy, stability and efficiency.

Finite volume methods are typically derived from the so called conservative form of a PDE. It is shown in Section 2.2.4, that the NSE equation can be brought to the conservative form. In general, the conservative form can be written as:

$$\frac{\mathrm{d}\boldsymbol{\xi}}{\mathrm{d}t} + \nabla \cdot f(\boldsymbol{\xi}) = \mathbf{0} \quad \texttt{eq:general\_conservative\_form} \tag{30}$$

(31)

where $\boldsymbol{\xi}$ represents a vector of states and f is the so-called flux tensor.
After subdividing the domain into finite volumes, also called cells, one can write for each particular cell i

$$\int_{V_i} \frac{\mathrm{d}\boldsymbol{\xi}}{\mathrm{d}t} dV_i + \int_{V_i} \nabla \cdot f(\boldsymbol{\xi}) dV_i \tag{32}$$

It shall be stressed again that reformulating the equations in integral form has already changed the space of admissible solutions. Particlularly, the integral form is capable of capturing discontinuities, like shocks whereas the derivative term would be undefined at a shock in equation (30).

After applying the divergence theorem to the second term this gives:

$$\frac{\mathrm{d}}{\mathrm{d}t} \int_{V_i} \boldsymbol{\xi} dV_i + \int_{\partial V_i} f(\boldsymbol{\xi}) \cdot \boldsymbol{n} \, dS_i \tag{33}$$

And after integration the first term to get the volume average

$$V_i \frac{\mathrm{d}\bar{\boldsymbol{\xi}}}{\mathrm{d}t} + \int_{\partial V_i} f(\boldsymbol{\xi}) \cdot \boldsymbol{n} \, dS_i \tag{34}$$

So that finally, the equation can be written as

$$\frac{\mathrm{d}\bar{\boldsymbol{\xi}}}{\mathrm{d}t} + \frac{1}{V_i} \int_{\partial V_i} f(\boldsymbol{\xi}) \cdot \boldsymbol{n} \, dS_i \quad \texttt{eq:final\_fv\_general} \tag{35}$$

which can easily be interpreted. The cell average of the conserved properties changes according to the total flux through the cells surface. Of course, the conservative value is defined as being constant within one cell, so there will be different values on faces or edges, depending on which side one is looking at. There are different approaches on how to choose an appropriate value. And the choice may greatly effect the numerical properties. In a FV solver, the numerical flux at the interface is typically constructed such, that upwinding is achieved.

3.2 Finite Volume method for fluid mechanics

It has already been shown in Section 2.2.4, that the NSE can be brought into the conservative form (12). The flux has been shown to consist of a convective and a diffusive part(16)(19). For this thesis, a Monotonic Upwind scheme for Conservation Laws (MUSCL) type FV framework for unstructured three-dimensional grids, as described in [8] has been used.

In equivalent manner as in equations (30) to (35) one can now write the conservative form of the NSE as

$$\frac{\partial \bar{\boldsymbol{w}}_i}{\partial t} + \frac{1}{\|\Omega_i\|}\int_{\partial\Omega_i} \mathcal{F}(\boldsymbol{w}) \cdot dS + \frac{1}{\|\Omega_i\|}\int_{\partial\Omega_i} \mathcal{G}(\bar{\boldsymbol{w}}, \nabla\bar{\boldsymbol{w}}) \cdot dS = \mathbf{0} \tag{36}$$

eq:NSE_full_FV_formulation

3.3 Mixed FV-FE formulation

It would be totally correct to now solve both terms with classical FV methods. However, we note two things. First, there is no need for upwinding in the diffusive term due to its elliptic nature. Secondly, the integration of the second term also becomes much more cumbersome than the first one to the gradient of the fluid state vector demanding at least a first order representation.
For this reasons, we introduce the following, mixed FV-FE formulation

$$\frac{\partial \boldsymbol{w}_i}{\partial t} + \int_{\partial\mathcal{C}_i} \mathcal{F}(\boldsymbol{w}) \cdot dS - \int_{\sum_{T_i}} \mathbb{K}\boldsymbol{w}\nabla\phi_i dx = \mathbf{0} \tag{37}$$

eq_mixed_FV_FE

where $\mathbb{K}$ is the diffusive tensor introduced in **TODO** and ϕ_i is a linear P1 shape-function over the triangle. Please also note that the convective term is now integrated over the dual cell related to vertex i, whereas the diffusive term integrated over all primal triangles connected to vertex i.
We will justify this re-formulation in section 3.4.

As can be seen from Figure 2, the dual cells themselves can have very random shapes. This makes the integration over the boundary of the second term in Equation (37) more cumbersome than in a primal approach. Also, the volume integral in the FE-like expression has to be splitted into regular shaped subdomains, e.g. tetrahedra, such that standard integration rules, like gauss-rule, can be applied.

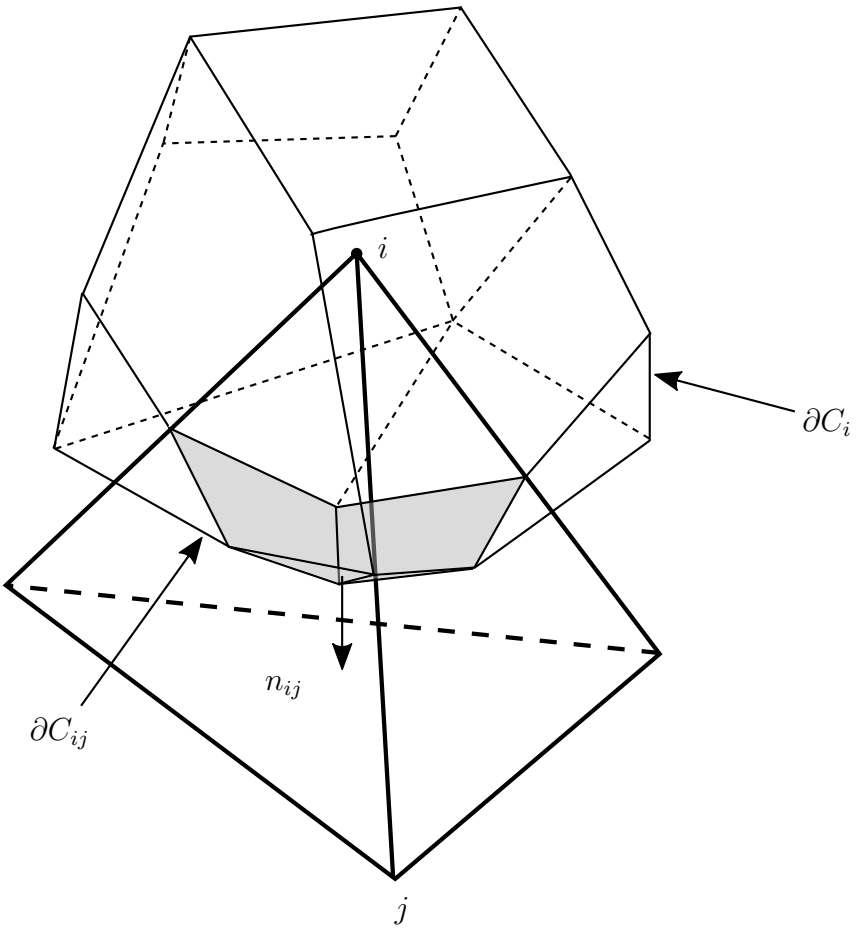

Figure 2: FV semi-discretization of an unstructured mesh. Vertex i is the center of dual cell C_i. The boundary of the dual cell is denoted as ∂C_{ij}

For a closer look into the convective fluxes integral, we decompose the boundary as $\partial\Omega_i = \sum_{i\in\kappa(i)} \partial\Omega_{ij}$, where $\kappa(i)$ denotes the set of vertices connected by an edge to vertex i.
In this thesis, the surface integral in equation (37) is than approximated using a Riemann solver and a MUSCL [15] technique. This approximation can be written as

$$\int_{\partial\Omega_i} \mathcal{F}(\boldsymbol{w}) \cdot dS \approx \sum_{j\in\kappa(i)} \boldsymbol{\phi}_{ij}(\boldsymbol{w}_{ij}, \boldsymbol{w}_{ji}, \boldsymbol{n}_{ij}) \tag{38}$$

eq:convectiveterm_approximation

where $\boldsymbol{\phi}_{ij}$ denotes the chosen numerical flux function along the edge $i-j$ and the two extrapolated fluid states at the i and the j-side of the the intersection of the cell boundary $\partial\Omega_{ij}$ and edge $i-j$ are denoted by $\boldsymbol{w}_{ij}$ and $\boldsymbol{w}_{ji}$ respectively. The area-weighted normal of edge $i-j$ is denoted as $\boldsymbol{n}_{ij}$.
A popular choice for the numerical approximation of the convective fluxes is the so-called Roe flux. Appropriate upwinding is directly built into the definition of the

Roe flux [?]. In 1D it is defined as:

$$\boldsymbol{\phi}_{ij} = \frac{1}{2}\left(\mathcal{F}(\mathbf{w}_j) + \mathcal{F}(\mathbf{w}_i)\right) - \frac{1}{2}|\mathbf{A}|\left(\mathbf{w}_j - \mathbf{w}_i\right) \tag{39}$$

To evaluate a roe-flux between two points in 2D or 3D, a normal vector is required to project the higher, dimensional flux on the connecting line.
As for the volume integral of the diffusive term in Equation (37), it shall be noted that the shape function is still denoted in the primal cell. Since the gradient of the test function is constant, as is the diffusive flux itself, the integral becomes a summation of the primal sub-tetrahedral contributions.

The final numerical approximation can therefore be summarized as

$$\frac{\partial \bar{\mathbf{w}}_i}{\partial t} + \sum_{j\in\kappa(i)} \boldsymbol{\phi}_{ij}(\mathbf{w}_{ij}, \mathbf{w}_{ji}, \boldsymbol{\nu}_{ij}) - \sum_{T_i\in\lambda(i)} \int_{T_i} \mathbb{K}\nabla\mathbf{w}\nabla\phi_i dx = \mathbf{0} \tag{40}$$

eq:nse_final_discretized

where $\kappa(i)$ is the set of vertices connected to vertex i by an edge, and $\lambda(i)$ is the set of primal elements connected to vertex i.

3.4 Derivation of the mixed FV-FE formulation

The equivalence of the finite volume representation of the viscous term, with the finite element-like representation provided in Equation (37) might not be obvious to the reader. This section is therefore denoted to a FE discretization of the governing equations, that can then be reformulated such that the mixed FV-FE formulation is obtained.
First, we start with the full NSE in conservative form, as provided in Equation (12). Next, a test function is defined. We chose the function $(\chi_i)_{i\in\mathcal{P}_h}$ where $\mathcal{P}_h$ represents the primal mesh, as step functions over the dual cells of $\mathcal{D}_h$. A multiplication with the test-functions and subsequent integration thus gives the following weak form

$$\int_\Omega \frac{\partial \boldsymbol{w}}{\partial t}\chi_i dx + \int_\Omega \nabla\cdot\mathcal{F}(\boldsymbol{w})\chi_i dx + \int_\Omega \nabla\cdot\mathcal{G}(\boldsymbol{w},\nabla\boldsymbol{w})\chi_i dx = \mathbf{0} \tag{41}$$

fv_weak_form_felike

(42)

where by using the divergence theorem, we obtain

$$\int_\Omega \nabla\cdot\mathcal{F}(\boldsymbol{w})\chi_i dx = \int_{\partial C_i} \mathcal{F}(\boldsymbol{w})\cdot\boldsymbol{n} ds \tag{43}$$

eq:divtheorem_felike

$$\int_\Omega \nabla\cdot\mathcal{G}(\boldsymbol{w},\nabla\boldsymbol{w})\chi_i dx = \underbrace{\int_{\partial C_i} \mathbb{K}\nabla\boldsymbol{w}\cdot\boldsymbol{n} ds}_{II} \tag{44}$$

Where the first term is already equivalent to what we have derived by the FV approach in (36).

It the diffusive tensor $\mathbb{K}$ is approximated to be constant over the triangle, which is justified in **TODO**, the product $\mathbb{K}\boldsymbol{w}$ is constant, one can now write the above integral as

$$II = \sum_{T\in\mathcal{D}_i} \mathbb{K}\nabla\boldsymbol{w}\int_{\partial C_i\cap T}\boldsymbol{n}_C ds \tag{45}$$

Now, we use a particular geometric relation, that holds for primitive elements like triangles and tetrahedra, and is derived in Section 3.4.1

$$\int_{C_i\cap T}\boldsymbol{n} ds = \frac{\boldsymbol{n}_i^T}{2} \tag{46}$$

where $\boldsymbol{n}_i^T$ is the normal to the primal mesh triangle T on the edge opposite of node i. This is where the geometric considerations of section 3.4.1 come into place. As shown in equations (55), the integral over the dual face edge can be written via the normal of the primal mesh triangle as

$$-\sum_{T\in\mathcal{D}_i}\mathbb{K}\nabla\boldsymbol{w}\frac{\boldsymbol{n}_i^T}{2} \tag{47}$$

Also, we have shown in Section 3.4.1, that for the case of a simple triangle (but equally applicable to tetrahedra), the last term of the above equation can be written as

$$-\sum_{T\in\mathcal{D}_i}\mathbb{K}\nabla\boldsymbol{w}\int_T\nabla\phi_i dx \tag{48}$$

where ϕ_i is the P1 shape-function defined in (50). Finally we can go the opposite way, and join the summations over integrals over triangular contributions back to an overall integral over the whole dual cell. Doing this finally leads to

$$II=-\int_{\mathcal{D}_i}\mathbb{K}\nabla\boldsymbol{w}\cdot\nabla\phi_i dx \tag{49}$$

which is exactly the term provided in equation (40). Since we used the same step-function based test-functions for all terms in equation (41), this approach is not only consistent, for the special case, of linear triangles we have shown that our finite element term is equivalent to a FV approximation.

3.4.1 Geometric considerations

This section is dedicated to the derivation of a particular link between the shape-function of a linear triangle/tetrahedra and its outward facing normals that we use in chapter 3.4 to proof the equivalence of the FE-formulation of the finite volume term with the FV formulation.

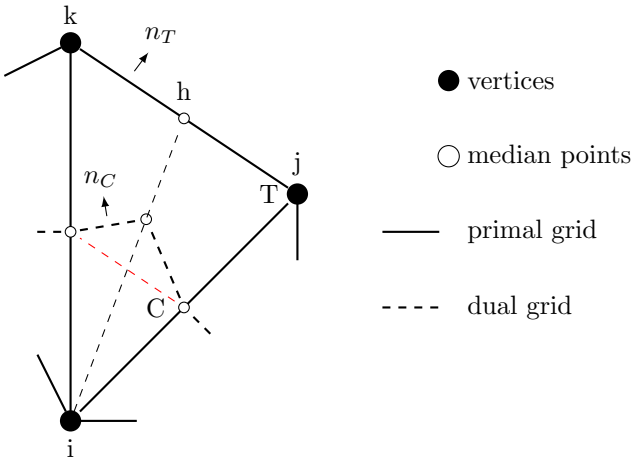

Figure 3: One Triangle T out of the set of triangles $\sum_T$, that are connected to vertex i. C denotes the dual cell related to vertex i.

We first look at one triangle of the set of triangles $\sum_T$ that belong to node i. The setup is visualized in Figure 3.
The reader can easily verify, that a linear shape-function of node i can be written as:

$$\phi_i(\boldsymbol{x})=\frac{\boldsymbol{hx}\cdot\boldsymbol{hi}}{\|\boldsymbol{hi}\|^2} \tag{50}$$ eq:p1_triangle_eq1

where $\boldsymbol{hx}$ is the vector from point h to any point x in the triangle, and $\boldsymbol{hi}$ is the vector from point h to point i. For this particular representation of the shape function, the gradient can be elegantly written as

$$\nabla\phi_i(\boldsymbol{x}) = \frac{\boldsymbol{hi}}{\|\boldsymbol{hi}\|^2} = \frac{\hat{\boldsymbol{hi}}}{\|\boldsymbol{hi}\|} \tag{51}$$ eq:p1_triangle_eq2

where $\hat{\boldsymbol{hi}}$ is the normalized vector in $h - i$ direction. Moreover, simple geometry tells us that

$$\|\boldsymbol{hi}\| \, \|\boldsymbol{kj}\| = 2|T| \tag{52}$$ eq:p1_triangle_eq3

where $|T|$ is the area of the triangle T

Substituting equation 52 into equation 51 therefore leads to

$$\nabla\phi_i(\boldsymbol{x}) = \boldsymbol{hi} \cdot \frac{\|\boldsymbol{kj}\|}{2|T|} = -\frac{\boldsymbol{\nu}}{2|T|} \tag{53}$$ eq:p1_triangle_eq4

where $\boldsymbol{\nu}$ is the weighted outward facing normal to edge jk.

$$\boldsymbol{\nu} = -\hat{\boldsymbol{hi}} \, \|kj\| = -\int_{[jk]} \boldsymbol{n}_T d\Gamma \tag{54}$$

Referring to previous chapter we remind the reader that in the vertex based FV approach, and integration over the dual face interface (dashed line in Figure 3) via the weighted interface normal is typically performed.

By simple geometrical considerations we can now determine, that the following relation holds

$$\int_{\Gamma_C \cap T} const. \; \boldsymbol{n}_c = \frac{1}{2} \int_{\Gamma_T} const. \; \boldsymbol{n}_T \tag{55}$$ eq:final_relation

$$= \frac{\boldsymbol{\nu_i^T}}{2} \tag{56}$$

4 Fluid structure interaction

Fluid Structure Interaction (FSI) describes the aeroelastic response of a mechanical system under fluid load, as well as the interaction between fluid and structure itself. Synonymously the term "Aeroelasticity" is often used.

For this thesis, we first will focus on an ALE formulation, a closer look into this topic in the context of en Embedded formulation will follow.

4.1 Coupled three-field formulation

In an aeroelastic ALE problem, three solution fields have to be considered. Firstly, the usual fluid problem has to be solved. Over the FSI interface, the fluid now interacts with the structure, imposing a Neumann problem on it. Finally, since we are considering ALE here, a governing equation for the fluid mesh motion has to be introduced, which closes the system.
Generally speaking, there exist two main approaches for solving this problem. Firstly, one can solve all three problems in one joint system, leading to a so-called monolithic algorithm. The advantage is, that the formulation is consistent and compared to the subsequently introduced staggered algorithm it does not introduce errors in the coupling. However, the solution of the monolithic system is cumbersome, since completely different physics are involved.
In practice, using a so-called "staggered algorithm" has shown to be a more robust choice. In a staggered algorithm, fluid- and structure problem are updated from time step n to $n+1$ one after the other. Therefore, consistency is lost, and (if no correction is applied) accuracy drops to first order. On the other hand each problem by itself can be treated by well established, optimized, existing solvers so the solution procedure is more robust.
This thesis utilizes the staggered approach. We have coupled a three-dimensional second order finite volume code [5] with a second order accurate finite element code[6] according to the popular three-field formulation of [3].

The three-field formulation of ALE aeroelasticity can be written as:

governing equation of structure:	$\mathcal{S}_{gov}(\boldsymbol{s}, \boldsymbol{u}, \boldsymbol{x}, \boldsymbol{w}) = \boldsymbol{0}$	eq:3field_structure (57)
governing equation of meshmotion:	$\mathcal{D}_{gov}(\boldsymbol{s}, \boldsymbol{u}, \boldsymbol{x}) = \boldsymbol{0}$	eq:3field_mesh (58)
governing equation of the fluid:	$\mathcal{F}_{gov}(\boldsymbol{s}, \dot{\boldsymbol{x}}, \boldsymbol{w}) = \boldsymbol{0}$	eq:3field_fluid (59)
		(60)

Governing equation of the structure: For a simple linear case, that is assumed in this thesis, the structure state equation can be written as

$$\mathcal{S}_{gov} = \mathbf{K}\boldsymbol{u} - \boldsymbol{P}(\dot{\boldsymbol{x}}, \boldsymbol{w}) \qquad \text{eq:eos\_struct} \quad (61)$$

where $\mathbf{K}$ represents the finite element stiffness matrix and $\boldsymbol{P}$ denotes the external load vector that combines aerodynamic loads $\boldsymbol{P}_F$ that are inflected to the structure by the fluid, and gravity loads $\boldsymbol{P}_0$

$$\boldsymbol{P} = \boldsymbol{P}_0 + \boldsymbol{P}_F \tag{62}$$

Governing equation of the mesh motion: In an Arbitrary Lagrangian Eulerian formulation, the fluid mesh deforms with the structure. A governing equation is thus required to describe that deformation. Typically a simple linear pseudo finite element approach or a spring analogy method [2] is used to do so. A Dirichlet problem is solved to move the mesh.

$$\mathcal{D}_{gov} = \bar{\mathbf{K}}\dot{\boldsymbol{x}} \quad \text{with} \quad \dot{\boldsymbol{x}} = \boldsymbol{u} \text{ on } \Gamma_{F|S} \tag{63}$$ eq:eos_mesh

Governing equation of the fluid: The state equation of the fluid depends on the flow model used, as well as on whether a Eulerian or Lagrangian approach is used. A quick overview is provided in Section 2.2.
Please note, that the frame of reference(Eulerian, Lagrangian, Arbitrary Lagrangian Eulerian) has nothing to do with the fluid equation type.

The state equation of the fluid(Equation three in (**??**)) can be expressed as

$$\mathcal{F}_{gov} = \begin{array}{|c|l|l|}\hline \multirow{3}{*}{Eulerian} & \text{Euler} & \frac{\partial \boldsymbol{w}}{\partial t} + \nabla \mathcal{F}(\boldsymbol{x}, \boldsymbol{w}) \\ \cline{2-3} & \text{NSE} & \frac{\partial \boldsymbol{w}}{\partial t} + \nabla \mathcal{F}(\boldsymbol{x}, \boldsymbol{w}) + \nabla \mathcal{G}(\boldsymbol{x}, \boldsymbol{w}) \\ \cline{2-3} & \text{RANS} & \frac{\partial \boldsymbol{w}}{\partial t} + \nabla \mathcal{F}(\boldsymbol{x}, \boldsymbol{w}) + \nabla \mathcal{G}(\boldsymbol{x}, \boldsymbol{w}) - \mathcal{S}(\boldsymbol{x}, \boldsymbol{w}, \boldsymbol{\chi}) \\ \hline \multirow{3}{*}{ALE} & \text{Euler} & \frac{\partial \boldsymbol{J}\boldsymbol{w}}{\partial t} + \boldsymbol{J}\nabla_\xi \mathcal{F}^c(\boldsymbol{x}, \dot{\boldsymbol{x}}, \boldsymbol{w}) \\ \cline{2-3} & \text{NSE} & \frac{\partial \boldsymbol{J}\boldsymbol{w}}{\partial t} + \boldsymbol{J}\nabla_\xi \mathcal{F}^c(\boldsymbol{x}, \dot{\boldsymbol{x}}, \boldsymbol{w}) + \boldsymbol{J}\nabla_\xi \mathcal{G}^c(\boldsymbol{x}, \dot{\boldsymbol{x}}, \boldsymbol{w}) \\ \cline{2-3} & \text{RANS} & \frac{\partial \boldsymbol{J}\boldsymbol{w}}{\partial t} + \boldsymbol{J}\nabla_\xi \mathcal{F}^c(\boldsymbol{x}, \dot{\boldsymbol{x}}, \boldsymbol{w}) + \boldsymbol{J}\nabla_\xi \mathcal{G}^c(\boldsymbol{x}, \dot{\boldsymbol{x}}, \boldsymbol{w}) - \mathcal{S}^c(\boldsymbol{x}, \dot{\boldsymbol{x}}, \boldsymbol{w}, \boldsymbol{\chi}) \\ \hline \end{array} = \mathbf{0} \tag{64}$$

where

$$\mathcal{F}^c(\boldsymbol{w}) = \mathcal{F}(\boldsymbol{w}) - \dot{\xi}\boldsymbol{w} \tag{65}$$

After FV discretization of the convective part, and FE discretization of the diffusive part, as explained in section **TODO**, the discrete system can be written as

$$\mathcal{F}_{gov} = \begin{array}{|c|l|l|}\hline \multirow{3}{*}{Eulerian} & \text{Euler} & \frac{\partial \mathbf{w}}{\partial t} + \mathbf{F}(\mathbf{x}, \mathbf{w}) \\ \cline{2-3} & \text{NSE} & \frac{\partial \mathbf{w}}{\partial t} + \mathbf{F}(\mathbf{x}, \mathbf{w}) + \mathbf{G}(\mathbf{x}, \mathbf{w}) \\ \cline{2-3} & \text{RANS} & \frac{\partial \mathbf{w}}{\partial t} + \mathbf{F}(\mathbf{x}, \mathbf{w}) + \mathbf{G}(\mathbf{x}, \mathbf{w}) - \mathbf{S}(\mathbf{x}, \mathbf{w}, \boldsymbol{\chi}) \\ \hline \multirow{3}{*}{ALE} & \text{Euler} & \frac{\partial \mathbf{A}(\mathbf{x})\mathbf{w}}{\partial t} + \mathbf{F}(\mathbf{x}, \dot{\mathbf{x}}, \mathbf{w}) \\ \cline{2-3} & \text{NSE} & \frac{\partial \mathbf{A}(\mathbf{x})\mathbf{w}}{\partial t} + \mathbf{F}(\mathbf{x}, \dot{\mathbf{x}}, \mathbf{w}) + \mathbf{G}(\mathbf{x}, \dot{\mathbf{x}}, \mathbf{w}) \\ \cline{2-3} & \text{RANS} & \frac{\partial \mathbf{A}(\mathbf{x})\mathbf{w}}{\partial t} + \mathbf{F}(\mathbf{x}, \dot{\mathbf{x}}, \mathbf{w}) + \mathbf{G}(\mathbf{x}, \dot{\mathbf{x}}, \mathbf{w}) - \mathbf{S}(\mathbf{x}, \dot{\mathbf{x}}, \mathbf{w}, \boldsymbol{\chi}) \\ \hline \end{array} = \mathbf{0} \tag{66}$$

Where we remind the reader that, as explained in section 3.2, for a FV discretization, the fluid state **w** has to be interpreted as average value over the cell. We often take the cell average to be equal to the value at the cell center, a n approximation that is second order accurate.

In the above equations **F** denotes the vector of Roe fluxes resulting from a second-order finite volume discretization of the convective part of the NSE, see section 3.2. Likewise, **G** likewise denotes an approximation of the diffusive part. As explained in section 3.3 we chose a FE approximation over a FV one for this term.
A denotes the matrix of cell volumes and **S** denotes the matrix resulting from the additional turbulence closures in the RANS equations (see Section 2.2.7).
The above table also gives a very nice overview over the different equation types and the used simplifications. The Euler equations are obviously obtained by neglecting the diffusive part of the NSE. One can also see that the RANS equations are more difficult than the NSE themselves. However, as explained in 2.2.7, the advantage is that RANS can operate on much coarser meshes that do not have to resolve the small scale turbulence phenomena, which makes them more numerically efficient overall in many applications.

4.1.1 Staggered algorithm

The three-field coupled system of equations (57)-(59), can be solved very efficiently with an iterative staggered procedure, such as the one proposed by by [3]. This work utilizes the second-order staggered algorithm described in Figure 4.

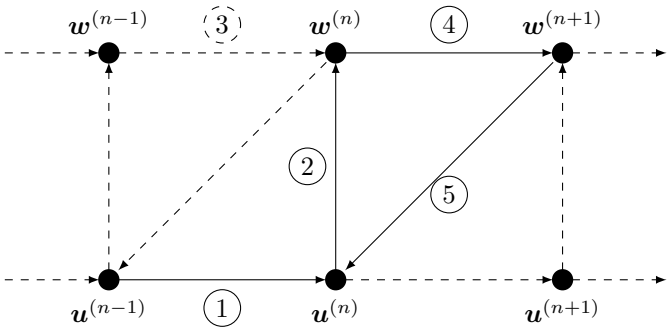

Figure 4: Scheme for the staggered algorithm. Th picture depicts the sequential structure($\boldsymbol{u}$) and fluid($\boldsymbol{w}$) solves. First, the structure is updated to a new time step. With this information, a corresponding fluid solution is obtained. After the fluid is progressed in time, the structure solutions is being corrected with that information. A detailed description of all steps follows below.

① Determining structural response For a given external load $\boldsymbol{P}^{(n)}$, the structural response $\boldsymbol{u}^{(n)}$ is determined by solving the state equation of the structure (57).

To increase stability, and under-relaxation is typically performed:

$$\boldsymbol{u}^{(n)} = (1-\theta)\boldsymbol{u}^{(n-1)} + \theta\tilde{\boldsymbol{u}} \tag{67}$$

$$\tilde{\boldsymbol{u}} = \mathbf{K}^{-1}\boldsymbol{P}^{(n)} \tag{68}$$

Typically, the relaxation factor is chosen as $0.5 \leq \theta \leq 0.9$

② Motion transfer to wet surface The motion of the wet surface of the structure has to be transformed to the fluid.

$$\boldsymbol{u}_T^{(n)} = \mathbf{T}_u\boldsymbol{u}^{(n)} \tag{69}$$

where $\mathbf{T}_u$ is a transfer matrix that also accounts for potentially non-matching meshes [9].

③ Fluid mesh motion update The fluid mesh motion is then updated by solving an auxiliary pseudo-Dirichlet problem on the fluid mesh. This step is at the very heart of the ALE algorithm.

$$\bar{\mathbf{K}}\dot{\boldsymbol{x}}^{(n)} = 0 \qquad \dot{\boldsymbol{x}}^{(n)} = \boldsymbol{u}_T^{(n)} \text{ on } \Gamma_{F|S} \tag{70}$$

where the Dirichlet conditions are introduced into the system via a decomposition:

$$\bar{\mathbf{K}} = \begin{bmatrix} \bar{\mathbf{K}}_{\Omega\Omega} & \bar{\mathbf{K}}_{\Omega\Gamma} \\ \bar{\mathbf{K}}_{\Gamma\Omega} & \bar{\mathbf{K}}_{\Gamma\Gamma} \end{bmatrix}, \quad \dot{\boldsymbol{x}} = \begin{bmatrix} \dot{\boldsymbol{x}}_\Omega \\ \dot{\boldsymbol{x}}_\Gamma \end{bmatrix} \tag{71}$$

Here, the subscript Γ denotes the fluid grid points at the FSI interface and the subscript Ω denotes the remainder. Hence, the fluid mesh is updated in two steps, by first transferring the structure motion to the fluid interface, and then solving the auxiliary pseudo Dirichlet problem:

$$\dot{\boldsymbol{x}}_\Gamma^{(n)} = \mathbf{T}_u\boldsymbol{u}^{(n)} \tag{72}$$ eq:mms_update_1

$$\bar{\mathbf{K}}_{\Omega\Omega}\dot{\boldsymbol{x}}_\Omega^{(n)} = -\bar{\mathbf{K}}_{\Omega\Gamma}\dot{\boldsymbol{x}}^{(n)} \tag{73}$$ eq:mms_update_2

It shall be noted that an exact solution of the preceding equation is not required. In fact it is an arbitrarily chosen auxiliary pseudo-problem anyway. Therefor, a valid update of the mesh motion, that does not produce crossovers is enough. Such an update can be obtained at low cost by allying a few Preconditioned Conjugate Gradient (PCG) iterations to Equation (73).

④ Update fluid state vector After the mesh has been deformed, the fluid state $\mathbf{w}$ vector can be updated by allying a singe Newton Rhapsodon iteration to

equation TODO, which leads to.

Eulerian	Euler	$\mathbf{F}(\mathbf{x}^{(n+1)}, \boldsymbol{w}^{(n)}) + \frac{\partial \mathbf{F}}{\partial \boldsymbol{w}}(\mathbf{x}^{(n+1)}, \boldsymbol{w}^{(n+1)} - \boldsymbol{w}^{(n)})$
	NSE	$< \text{term above} > + \frac{\partial \mathbf{G}}{\partial \boldsymbol{w}}(\mathbf{x}^{(n+1)}, \boldsymbol{w}^{(n+1)} - \boldsymbol{w}^{(n)})$
	RANS	$< \text{term above} > - \frac{\partial \mathbf{S}}{\partial \boldsymbol{w}}(\mathbf{x}^{(n+1)}, \boldsymbol{w}^{(n+1)} - \boldsymbol{w}^{(n)}, \boldsymbol{\chi})$
ALE	Euler	$\mathbf{F}(\mathbf{x}^{(n+1)}, \dot{\mathbf{x}}^{(n+1)}, \boldsymbol{w}^{(n)}) + \frac{\partial \mathbf{F}}{\partial \boldsymbol{w}}(\mathbf{x}^{(n+1)}, \dot{\mathbf{x}}^{(n+1)}, \boldsymbol{w}^{(n+1)} - \boldsymbol{w}^{(n)})$
	NSE	$< \text{term above} > + \frac{\partial \mathbf{G}}{\partial \boldsymbol{w}}(\mathbf{x}^{(n+1)}, \dot{\mathbf{x}}^{(n+1)}, \boldsymbol{w}^{(n+1)} - \boldsymbol{w}^{(n)})$
	RANS	$< \text{term above} > - \frac{\partial \mathbf{S}}{\partial \boldsymbol{w}}(\mathbf{x}^{(n+1)}, \dot{\mathbf{x}}^{(n+1)}, \boldsymbol{w}^{(n+1)} - \boldsymbol{w}^{(n)}, \boldsymbol{\chi})$

$$= 0 \quad (74)$$

is this correct? What do I do with the turbulence parameter?

⑤ Determining structural responses Once the new fluid-state vector has been determined, the pressure $p^{(n+1)}$ can be recovered. The pressure on the fluid interface side, than mifht need to be transfered to the structure via a transfer matrix $\mathbf{T}_u$ to account for potentially non-matching fluid-structure interfaces.

5 Optimization

A generic, aeroelastic optimization problem can be written as

$$q(\boldsymbol{s},\boldsymbol{u},\boldsymbol{w}) \begin{cases} \min\limits_{\boldsymbol{s}} z(\boldsymbol{s}) \\ \boldsymbol{h}(s)=\boldsymbol{0}, \quad \boldsymbol{h}\in\mathbb{R}^{n_h} \\ \boldsymbol{g}(s)>\boldsymbol{0}, \quad \boldsymbol{g}\in\mathbb{R}^{n_g} \end{cases} \tag{75}$$ eq:generic_optimization_problem_1

$$\boldsymbol{s}=\{\boldsymbol{s}\in\mathbb{R}^{n_s} | \boldsymbol{s}_L\leq\boldsymbol{s}\leq\boldsymbol{s}_U\} \tag{76}$$ eq:generic_optimization_problem_2

Here, z is an arbitrary cost function that should be minimized. Note that a maximization problem can easily be obtained by multiplying the cost function by a factor of -1. In aerodynamics, a typical example for a cost function would be the Lift over Drag Ratio (LDR) ratio of an airfoil. The cost-function is described in terms of so-called *abstract variables*. These can have some physical interpretation, but don't necessarily have to(see Section 5.2). Since typically, these optimization problems have no finite solution on an unbounded domain, some restrictions/conditions are introduced. In the airfoil example, we would probably specify a minimum lift that is required to support the configuration. Also a maximum stress for the structure will likely have to be specified. These are classical examples of non-equality constraints, denoted by $\boldsymbol{g}(\boldsymbol{s})$ in the above formulation. Constraints can also be formulated in an equality sense, for instance geometrical restrictions due to the turbine suspensions. Furthermore, the abstract optimization variables $\boldsymbol{s}$ themselves are typically restricted by lower($\boldsymbol{s}_L$) and upper($\boldsymbol{s}_U$) bounds.
The combinations of objective function z and constraints $\boldsymbol{h}$ and $\boldsymbol{g}$ is typically denoted as optimization criteria q.

$$\begin{aligned} q &= q(\boldsymbol{s},\boldsymbol{u},\boldsymbol{w}) \\ \boldsymbol{u} &= \boldsymbol{u}(\boldsymbol{s}), \quad \boldsymbol{w}=\boldsymbol{w}(\boldsymbol{s}) \end{aligned} \tag{77}$$ eq:optimization_criteria

This thesis follows the *nested analysis and design approach*, meaning that we assume that $\boldsymbol{u}$ and $\boldsymbol{w}$ always satisfy the aeroelastic state equations. This means that the state equations are not included in the set of constraints, but the structural displacements $\boldsymbol{u}$ and the fluid state variables $\boldsymbol{w}$ are determined in each iteration.

As [9] write, the aeroelastic optimization problem can typically be solved by combining three different numerical approaches:

- Optimization Model
- Design Model
- Analysis Model

The optimization model describes the solution of the generic optimization problem(75)-(76). For this thesis, a Sequential Quadratic Programming (SQP) has been chosen [4].
The design model links abstract optimization variables $\boldsymbol{s}$ to actual shapes, structures, geometries or aerodynamics design parameters. For this purpose SDESIGN, a

programm specifically written for SA purpose in the Farhat Research Group (FRG), has been used during this thesis. Its basic concepts an ideas are described in [10]. Finally, the analysis model provides concepts of evaluation the optimization criteria. Typically, the optimization criteria depend on $\boldsymbol{u}$ and $\boldsymbol{w}$ which is why a coupled system of equations has to be solved in every design optimization process. The Sensitivity Analysis (SA) is also part of this model. Aeroelastic analysis and Sensitivity analysis are discussed in Section 7.

5.1 Optimization Model

Optimization problems are typically solved by gradient-based methods. The methods are divided into

- Primal
- Dual
- Penalty-barrier and
- Lagrange approaches

This thesis focuses on Lagrange approaches. For a thorough analysis and comparison of the different approaches, the interested reader is referred to [12].
The Lagrangian approach formulates the optimization problem(75)(76) as an extreme value problem of the Lagrangian:

$$L(\boldsymbol{s}, \boldsymbol{\eta}, \boldsymbol{\gamma}) = z(\boldsymbol{s})) = \boldsymbol{\eta}^T \boldsymbol{h}(\boldsymbol{s}) + \boldsymbol{\gamma}^T \boldsymbol{g}(\boldsymbol{s}) \tag{78}$$

eq:lagrangian_of_optimization

$$\tag{79}$$

Here, $\boldsymbol{\eta}$ denote the Lagrange multipliers for the equality constraints and $\boldsymbol{\gamma}$ the Lagrange multipliers for the non-equality constraints. In fact, one can easily see that the original optimization problem can be obtained as saddle point of the Lagrangian:

$$\frac{\partial L}{\partial \boldsymbol{s}} = \frac{\partial z}{\partial \boldsymbol{s}} = \boldsymbol{\eta}^T \frac{\partial \boldsymbol{h}}{\partial \boldsymbol{s}} + \boldsymbol{\gamma}^T \frac{\partial \boldsymbol{g}}{\partial \boldsymbol{s}} \tag{80}$$

eq:saddlepoint_optimization

$$\frac{\partial L}{\partial \boldsymbol{\eta}} = \boldsymbol{h} = \boldsymbol{0} \tag{81}$$

$$\frac{\partial L}{\partial \boldsymbol{\gamma}} = \boldsymbol{\gamma}^T \boldsymbol{g} = \boldsymbol{0} \tag{82}$$

The SQP method, mention before uses a Newton-Rhapsodon algorithm to solve the above system.

$$\begin{bmatrix} \frac{\partial^2 L}{\partial \boldsymbol{s}^2}^{(k)} & \frac{\partial \boldsymbol{g}}{\partial s}^{(k)} & \frac{\partial \boldsymbol{h}}{\partial s}^{(k)} \\ \boldsymbol{\gamma}^{(k)} \frac{\partial \boldsymbol{g}}{\partial s}^{(k)} & \boldsymbol{h}^{(k)} & \boldsymbol{0} \\ \frac{\partial \boldsymbol{h}}{\partial s}^{(k)} & \boldsymbol{0} & \boldsymbol{0} \end{bmatrix} \begin{bmatrix} \Delta \boldsymbol{s} \\ \Delta \boldsymbol{\gamma} \\ \Delta \boldsymbol{\eta} \end{bmatrix} = - \begin{bmatrix} \frac{\partial L}{\partial \boldsymbol{s}}^{(k)} \\ \boldsymbol{\gamma}^{(k)T} \boldsymbol{g}^{(k)} \\ \boldsymbol{h}^{(k)} \end{bmatrix} \tag{83}$$

eq:saddlepoint_newtonform

Here $(\cdot)^{(k)}$ denotes the iteration index of the optimization loop.

The linear Equations (83) can also be formulated as an equivalent quadratic minimization problem:

$$\min_{\boldsymbol{s}} \left(\frac{1}{2}\Delta \boldsymbol{s}^T \frac{\partial^2 L}{\partial \boldsymbol{s}^2}^{(k)} \Delta \boldsymbol{s} + \frac{\partial L}{\partial \boldsymbol{s}}^{(k)}\right) \qquad \texttt{eq:quadratic\_minimization\_problem\_1} \tag{84}$$

$$\frac{\partial \boldsymbol{g}}{\partial s}^{(k)} \Delta \boldsymbol{s} + \boldsymbol{g}^{(k)} \geq \boldsymbol{0} \qquad \texttt{eq:quadratic\_minimization\_problem\_2} \tag{85}$$

$$\frac{\partial \boldsymbol{h}}{\partial s}^{(k)} \Delta \boldsymbol{s} + \boldsymbol{h}^{(k)} = \boldsymbol{0} \qquad \texttt{eq:quadratic\_minimization\_problem\_3} \tag{86}$$

In the above formulation, the evaluation of the second derivative of the Lagrangian(Hessian of L) is the numerically most expensive part. Usually it is preferred to approximate it by a first-order information, for example by the Davidon-Fletcher Powell formula (DFP) or by the Broyden-Fletcher-Goldfarb-Shanno algorithm (BFGS) method. However, this simplification introduces an error that one should be aware of. Some correction methods have been proposed trying to minimize the error. In this thesis we adapt the one proposed by [9]:

$$\begin{bmatrix} \boldsymbol{s}^{(k+1)} \\ \boldsymbol{\eta}^{(k+1)} \\ \boldsymbol{\gamma}^{(k+1)} \end{bmatrix} = \begin{bmatrix} \boldsymbol{s}^{(k)} \\ \boldsymbol{\eta}^{(k)} \\ \boldsymbol{\gamma}^{(k)} \end{bmatrix} + \alpha^{(k)} \begin{bmatrix} \Delta \boldsymbol{s}^{(k)} \\ \Delta \boldsymbol{\eta}^{(k)} \\ \Delta \boldsymbol{\gamma}^{(k)} \end{bmatrix} \qquad \texttt{eq:correction\_step} \tag{87}$$

The appropriate step size $\alpha^{(k)}$ is determined by a line search. AS [9] write, due to this insufficiencies, the Lagrangian can not be used to measure an improvement. Instead, a merit function is introduced that is minimized by the line-search. A local minimum is reached by following a sequence of decreasing merit function values. Convergence of the process can be measured via the $\mathcal{L}_2$-norm of the residual of the Kuhn-Tucker conditions(80).
By construction, the constraints are satisfied only when the optimum point is reached.

5.2 Design Model

The design model represent the essential link between the described optimization model and the analysis model. Generally speaking, it relates physical design parameters to abstract ones.

$$\boldsymbol{d} = \boldsymbol{d}(\boldsymbol{s}), \quad \boldsymbol{d} \in \mathbb{R}^{n_{\boldsymbol{d}}} \qquad \texttt{eq:physvarsTOabsvars} \tag{88}$$

Here, $n_{\boldsymbol{d}}$ denotes the number of physical design parameters. To define a relation between the abstract optimization variables and the motion of the nodes, the following design model is introduced:

$$\dot{\boldsymbol{x}} = \dot{\boldsymbol{x}}(\boldsymbol{s}) \tag{89}$$

As [9] explain, it is unpractical to identify an abstract variable directly with an increment of the coordinate of a grid point. Instead, two approaches, namely geometrical and mechanical can be adopted for constructing the generic design model.

Mechanical approach In the mechanical approach, the shape variation is identified with a superposition of fictitious structural deformations $\bar{\boldsymbol{u}}_j$ due to fictitious loads $\mu\bar{\boldsymbol{P}}_j$ and fictions support conditions

$$\dot{\boldsymbol{x}} = \sum_j \bar{\boldsymbol{u}}_j = \sum_j \bar{\mathbf{K}}_j^{-1} \mu_j \bar{\boldsymbol{P}}_j \tag{90}$$ eq:mechanical_approach

where $\bar{\mathbf{K}}_j$ is a fictitious pseudo structure stiffness matrix representing the fluid domain compatible to the current fictions support conditions.

Geometrical approach The geometrical approach describes the geometry of the structure or the fluid boundary the design element concept. Here, the shape of a body $\boldsymbol{X}$ is approximated by so-called design elements as follows:

$$\boldsymbol{X} = \sum_j \phi_j(\xi) \hat{\boldsymbol{X}}_j \tag{91}$$ eq:geometrical_approach

Here, $\phi_j(\xi)$ is a shape function, $\hat{\boldsymbol{X}}_j$ is the vector of control nodes and ξ represents the reference coordinate. In the design element concept, the variation of the control nodes of the design element is used to vary the shape of the body. The variation of the control nodes position denoted as "mesh-motion" is given as $\dot{\boldsymbol{x}} = \Delta\hat{\boldsymbol{X}}$

$$\dot{\boldsymbol{x}} = \sum_j \phi_j(\xi) \hat{\dot{\boldsymbol{x}}}_j \tag{92}$$ eq:mms

Just as in Finite Elements, where the shape-functions can not only be used to describe the solution field, but also the body's geometry and material parameters, the design element concept can be applied to prescribe parameter distributions and their variations in the optimization process. A simple sketch of the concept is provided in Figure 5
Both approaches have pros and cons, that are quickly discussed in [10], this thesis utilizes the geometrical approach solemnly.

5.3 Analysis Model

In the analysis model, the optimization criteria q are determined for a given set of obtimization variables s. Since the optimization algorithm choses in this thesis is

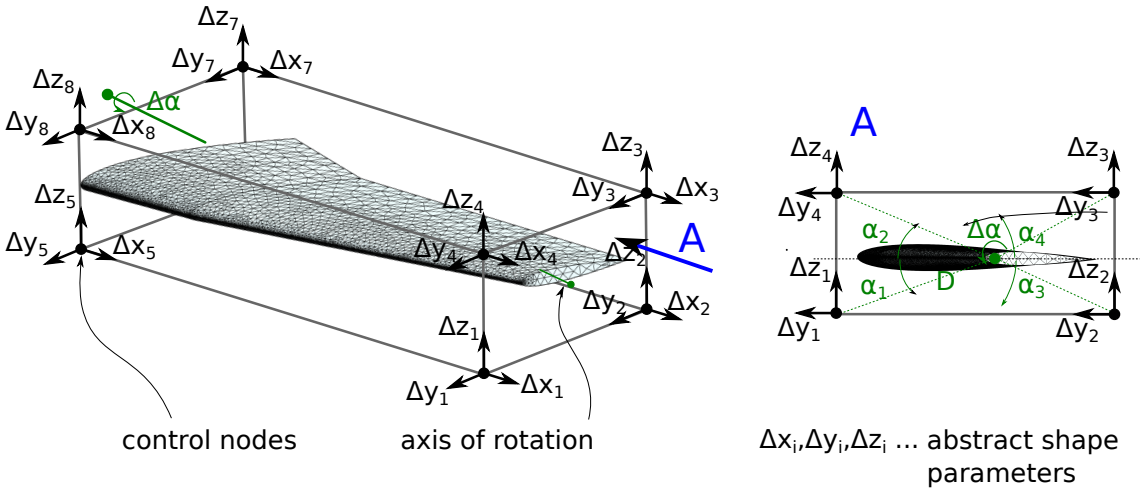

Figure 5: Geometrical approach for the design model as explained in Section 5.2. A NACA type airfoil is considered here as an example. The airfoil is embedded in a bounding box defined by eight so-called control nodes. The position of these control nodes can be varied, which alternates the shape of the airfoil according to some interpolation functions defined on the nodes. The 24 displacement unknowns are denoted as "abstract shape parameters". Abstract shape variables can be arbitrarily defined. As an example, a rotation axis is defined through the wing.

based on gradients, the gradients of the optimization criteria with respect to the abstract variables are determined in this step. A main focus on this thesis has been the appropriate evaluation of these derivatives, we therfore denote the subsequent chapter 6 to the issue.

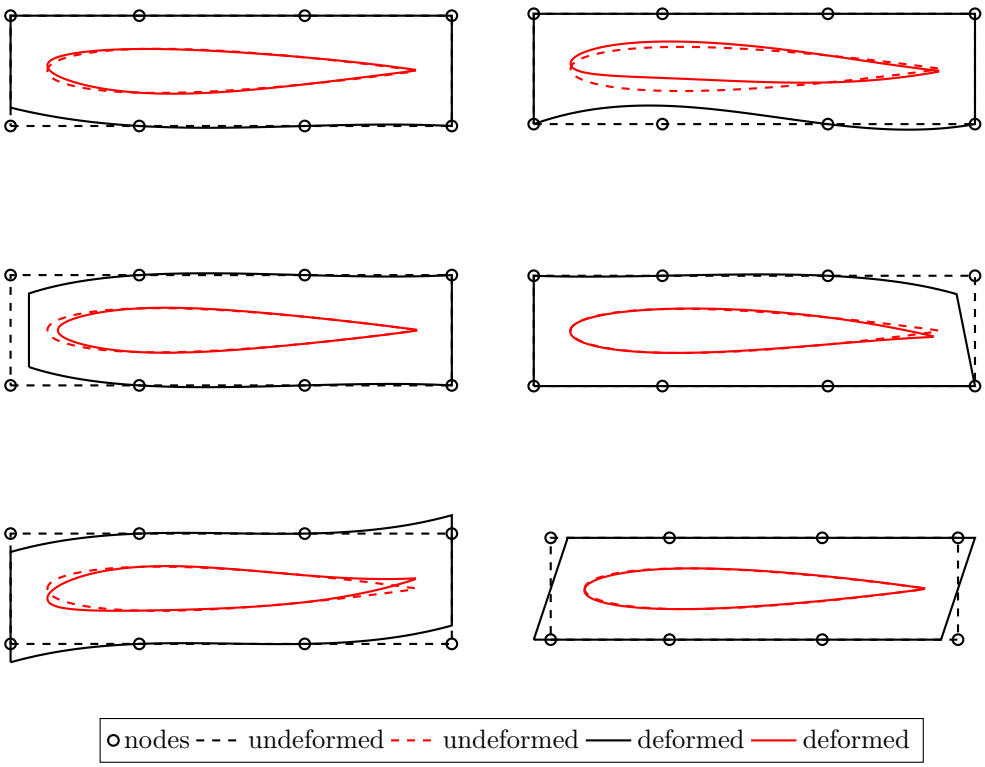

Figure 6: Visualization of the design element concept, exemplarily shown on a NACA0012 airfoil. For simplicity, a single design element(cubic in the horizontal direction and linear in the vertical direction) is used. Both the initial configuration(dashed lines) and the deformed configuration(full lines) are plotted. Although only eight design element nodes are provided, the function space of the design element allows for a great variation of the airfoil shape. Also, the size of the parameter space is now independent of the airfoil mesh size. From this perspective, the design element concept can be regarded as an model reduction for the shape variation.

6 Fluid Sensitivity Analysis (SA)

As explained in section 5, optimization is based on the calculations of gradients, also denoted as Sensitivity Analysis (SA). When it comes to calculating the gradients of a solution of a PDE, there are two fundamentally different approaches one could take.
Firstly one could think of first deriving the continous equation and then applying the discretization scheme. On the other hand its equaly legitimate to first apply the discretization and compute the gradients of that, approximated solution. This thesis focuses uses the latter one, the reasons being explained in Figure 7.

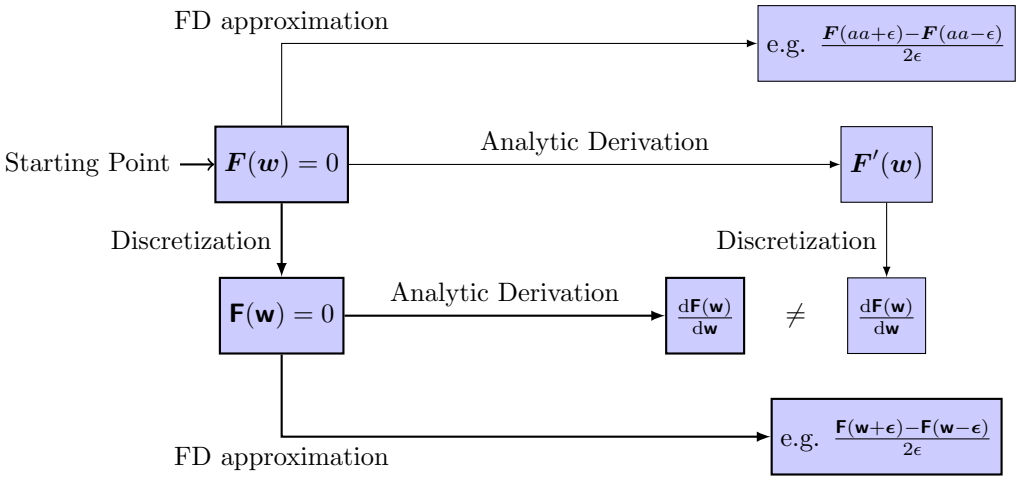

Figure 7: Two different approaches of SA. The question here is whether to discretize the system of equations first and then compute the derivatives of the approximate solution, or whether the continuous system of equation is first derived and discretized afterwards. Both approaches are valid, the final result however will generally not be the same. We have solemnly focused on the case of derivation after discretization in this thesis(thick lines). There are several reason to this. Firstly, if one chose to first derive and then compute a discretized solution, one would solve a completely different equation. If on the other hand the discretization(e.g. Finite Volumes) is done first, standard solvers can be utilized. What is more, approximating the derivative by a Finite difference becomes much easier, since the finite difference evaluation involves only a evaluation of $\mathbf{F}$*, which a standard fluid solver is perfectly capable of, whereas the FD approximation in the other case would involve evaluations of the continuous function and the discretization of the obtained expression which would be much more cumbersome.* ***Think about whether this is correct***

When it comes to SA within the context of CFD, one also has to distinguish between SA of the non-coupled fluid problem and the SA in the fully coupled aeroelastic case. The latter case is much more involved, since it requires additional terms from the Structure and mesh motion equations. In the following we will therefore begin with the SA of a regular fluid problem. A generalization to a coupled FSI problem will follow.

As mentioned in Section 5, we typically deal with an optimization criteria q_j, that is in this case dependent on the fluid state variables $\boldsymbol{w}$ that themselves may depend on abstract variables s_i

$$q_j = q_j(\boldsymbol{w}(s_i)) \tag{93}$$

$$\left.\frac{dq_j}{ds_i}\right|_{\boldsymbol{w}_0} = \underbrace{\left.\frac{\partial q_j}{\partial s_i}\right|_{\boldsymbol{w}_0}}_{\substack{\text{directy derived from} \\ \text{the definition of } q}} + \underbrace{\left.\frac{\partial q_j}{\partial \boldsymbol{w}}\right|_{\boldsymbol{w}_0}}_{\substack{\text{derived analytically or} \\ \text{by FD}}} \underbrace{\left.\frac{d\boldsymbol{w}}{ds_i}\right|_{\boldsymbol{w}_0}}_{\substack{\text{derived from dynamic} \\ \text{fluid equilibrium}}} \tag{94}$$

Also, we keep in mind, that the state equation of the fluid can be expressed as

$$\mathcal{F}_{gov}(\boldsymbol{w}(s_i), \dot{\boldsymbol{x}}(s_i), s_i) = \frac{\partial \boldsymbol{w}(s_i)}{\partial t} + \nabla \cdot \mathcal{F}(\boldsymbol{w}(s_i)) + \nabla \mathcal{G}(\boldsymbol{w}(s_i)) + S = \mathbf{0} \tag{95}$$

TODO how does the mesh motion come into the right hand side?

Therefore, deriving the fluid EOS gives:

$$\frac{\mathrm{d}\mathcal{F}_{gov}}{\mathrm{d}s_i} = \mathbf{0} = \frac{\partial \mathcal{F}_{gov}}{\partial s_i} + \frac{\partial \mathcal{F}_{gov}}{\partial \boldsymbol{w}}\frac{d\boldsymbol{w}}{ds_i} + \frac{\partial \mathcal{F}_{gov}}{\partial \dot{\boldsymbol{x}}}\frac{d\dot{\boldsymbol{x}}}{ds_i} \tag{96}$$

Therefore the total derivative of the fluid state with respect to the shape variable, needed in equation REF, can be obtained by solving

$$\frac{\partial \mathcal{F}_{gov}}{\partial \boldsymbol{w}}\frac{d\boldsymbol{w}}{ds_i} = -\frac{\partial \mathcal{F}_{gov}}{\partial s_i} - \frac{\partial \mathcal{F}_{gov}}{\partial \dot{\boldsymbol{x}}}\frac{d\dot{\boldsymbol{x}}}{ds_i} \tag{97}$$

In this equation, $\dfrac{\partial \mathcal{F}_{gov}}{\partial s_i}$ can be computed analytically or by FD. The derivative of the mesh motion with respect to the abstract variables is often denoted as "shape gradient". It can be divided into two components:

- The interface component $\dfrac{\mathrm{d}\dot{\boldsymbol{x}}_\Gamma}{\mathrm{d}s_i}$, which is associated with the grid points lying on the fluid boundary
- The interior component $\dfrac{\mathrm{d}\dot{\boldsymbol{x}}_\Omega}{\mathrm{d}s_i}$, which is associated with the grid points located in the interior Ω of the computational domain.

The interface component is determined by the structure. Having obtained this one, the interior component can be computed by solving an auxiliary, fictitious Dirichlet problem:

$$\frac{\mathrm{d}\dot{\boldsymbol{x}}_\Omega}{\mathrm{d}s_i} = -\left[\bar{\mathbf{K}}_{\Omega\Omega}^{-1}\bar{\mathbf{K}}_{\Omega\Gamma}\right]\frac{\mathrm{d}\dot{\boldsymbol{x}}_\Gamma}{\mathrm{d}s_i} \tag{98}$$

where $\bar{\mathbf{K}}$ is a pseudo stiffness matrix that can be obtained by a simple spring analogy or similar approaches. For the later introduced Embedded framework, $\frac{\mathrm{d}\dot{\boldsymbol{x}}}{\mathrm{d}s_i}$ is the position vector of the embedded discrete surface
In summary, the derivative of an optimization criteria with respect to an abstract variable can be computed as

$$\left.\frac{\mathrm{d}q_j}{\mathrm{d}s_i}\right|_{\boldsymbol{w}_0} = -\left.\frac{\mathrm{d}q_j}{\mathrm{d}\boldsymbol{w}}\right|_{\boldsymbol{w}_0}\left[\left.\frac{\partial \mathcal{F}_{gov}}{\partial \boldsymbol{w}}\right|_{\boldsymbol{w}_0}\right]^{-1}\left(\left.\frac{\partial \mathcal{F}_{gov}}{\partial s_i}\right|_{\boldsymbol{w}_0} + \left[\left.\alpha\frac{\partial \mathcal{F}_{gov}}{\partial \dot{\boldsymbol{x}}_\Omega}\right|_{\boldsymbol{w}_0} \left.\frac{\partial \mathcal{F}_{gov}}{\partial \dot{\boldsymbol{x}}_\Gamma}\right|_{\boldsymbol{w}_0}\right]\begin{bmatrix}\alpha\bar{\mathbf{K}}_{\Omega\Omega}^{-1}\bar{\mathbf{K}}_{\Omega\Gamma}\\ \mathbf{I}\end{bmatrix}\frac{\mathrm{d}\dot{\boldsymbol{x}}_\Gamma}{\mathrm{d}s_i}\right) \tag{99}$$

eq:full_sa_nostruct

$$\alpha = \begin{cases} 1 \text{ in ALE framework} \\ 0 \text{ in Embedded framework} \end{cases} \tag{100}$$

7 Aero-elastic Sensitivity Analysis

The SA approach applied in this thesis is based on the work of [14], for deriving the Global Sensitivity Equations (GSE) of coupled systems. As introduced by the authors of[9], we utilize the three-field formulation of [3].

The derivative of the optimization criterion q_j, as introduced in Equation (77), with respect to the optimization variable s_i gives:

$$\frac{dq_j}{ds_i} = \frac{\partial q_j}{\partial s_i} + \frac{\partial q_j}{\partial \boldsymbol{u}}\frac{d\boldsymbol{u}}{ds_i} + \frac{\partial q_j}{\partial \dot{\boldsymbol{x}}}\frac{d\dot{\boldsymbol{x}}}{ds_i} + \frac{\partial q_j}{\partial \boldsymbol{w}}\frac{d\boldsymbol{w}}{ds_i} \tag{101}$$

$$= \frac{\partial q_j}{\partial s_i} + \begin{bmatrix} \frac{\partial q_j}{\partial \boldsymbol{u}} \\ \frac{\partial q_j}{\partial \dot{\boldsymbol{x}}} \\ \frac{\partial q_j}{\partial \boldsymbol{w}} \end{bmatrix}^T \cdot \begin{bmatrix} \frac{d\boldsymbol{u}}{ds_i} \\ \frac{d\dot{\boldsymbol{x}}}{ds_i} \\ \frac{d\boldsymbol{w}}{ds_i} \end{bmatrix} \tag{102}$$

where the partial derivatives, $\frac{\partial q_j}{\partial \boldsymbol{u}}$, $\frac{\partial q_j}{\partial \dot{\boldsymbol{x}}}$ and $\frac{\partial q_j}{\partial \boldsymbol{w}}$ can be directly evaluated within the discretized structure and fluid model through the relation between structural, aerodynamic design and abstract optimization parameters defied in the design model 5.2. The cumbersome part are the derivatives $\frac{d\boldsymbol{u}}{ds_i}$, $\frac{d\dot{\boldsymbol{x}}}{ds_i}$ and $\frac{d\boldsymbol{w}}{ds_i}$ To obtain them, the governing equations (**??**)**TODO write down governing equations** have to be derived:

$$\begin{bmatrix} \frac{\partial \mathcal{S}_{gov}}{\partial s_i} \\ \frac{\partial \mathcal{D}_{gov}}{\partial s_i} \\ \frac{\partial \mathcal{F}_{gov}}{\partial s_i} \end{bmatrix} + \underbrace{\begin{bmatrix} \frac{\partial \mathcal{S}_{gov}}{\partial \boldsymbol{u}} & \frac{\partial \mathcal{S}_{gov}}{\partial \dot{\boldsymbol{x}}} & \frac{\partial \mathcal{S}_{gov}}{\partial \boldsymbol{w}} \\ \frac{\partial \mathcal{D}_{gov}}{\partial \boldsymbol{u}} & \frac{\partial \mathcal{D}_{gov}}{\partial \dot{\boldsymbol{x}}} & \boldsymbol{0} \\ \boldsymbol{0} & \frac{\partial \mathcal{F}_{gov}}{\partial \dot{\boldsymbol{x}}} & \frac{\partial \mathcal{F}_{gov}}{\partial \boldsymbol{w}} \end{bmatrix}}_{\boldsymbol{A}} \begin{bmatrix} \frac{\partial \boldsymbol{u}}{\partial s_i} \\ \frac{\partial \dot{\boldsymbol{x}}}{\partial s_i} \\ \frac{\partial \boldsymbol{w}}{\partial s_i} \end{bmatrix} = \boldsymbol{0} \tag{103}$$

eq:governing_equations_derivative

In this equations $\frac{\partial \mathcal{S}_{gov}}{\partial s_i}$ and $\frac{\partial \mathcal{F}_{gov}}{\partial s_i}$ can be again directly evaluated using the relation specified in the design model. The matrix of first derivatives $\boldsymbol{A}$ is from now on denoted as the "Jacobian of the optimization problem".
Combining the previous two equations, it follows that the total derivative of the

optimization criterion with respect to the abstract variables can be expressed as:

$$\frac{dq_j}{ds_i} = \frac{\partial q_j}{\partial s_i} - \underbrace{\begin{bmatrix} \frac{\partial q_j}{\partial \boldsymbol{u}} \\ \frac{\partial q_j}{\partial \dot{\boldsymbol{x}}} \\ \frac{\partial q_j}{\partial \boldsymbol{w}} \end{bmatrix}^T}_{n_{\boldsymbol{q}} \times n_{eq}} \underbrace{\boldsymbol{A}^{-1}}_{n_{eq} \times n_{eq}} \underbrace{\begin{bmatrix} \frac{\partial \mathcal{S}_{gov}}{\partial s_i} \\ \frac{\partial \mathcal{D}_{gov}}{\partial s_i} \\ \frac{\partial \mathcal{F}_{gov}}{\partial s_i} \end{bmatrix}}_{n_{eq} \times n_{\boldsymbol{s}}} \quad \texttt{eq:totderiv\_optcritBYabsvar} \tag{104}$$

Where n_{eq} is the total number of equations(e.g. five fluid state equations for the compressible NSG in 3D, three equations of the mesh motions and another three equations for the structure motion), n_q is the number of optimization criteria and n_s is the number of abstract variables.

7.1 Direct vs. adjoint approach

Equation 104 suggests, that there are two alternatives to compute vector-matrix-vector product above.

Direct approach Firstly, one could first compute the derivatives of the aeroelastic response for each abstract variable and perform the matrix product with $\boldsymbol{A}$:

$$\begin{bmatrix} \frac{d\boldsymbol{u}}{ds_i} \\ \frac{d\dot{\boldsymbol{x}}}{ds_i} \\ \frac{d\boldsymbol{w}}{ds_i} \end{bmatrix} = -\boldsymbol{A}^{-1} \begin{bmatrix} \frac{\partial \mathcal{S}_{gov}}{\partial s_i} \\ \frac{\partial \mathcal{D}_{gov}}{\partial s_i} \\ \frac{\partial \mathcal{F}_{gov}}{\partial s_i} \end{bmatrix} \quad \text{and then} \quad \texttt{eq:direct\_approach} \tag{105}$$

$$\frac{dq_j}{ds_i} = \frac{\partial q_j}{\partial s_i} - \begin{bmatrix} \frac{\partial q_j}{\partial \boldsymbol{u}} \\ \frac{\partial q_j}{\partial \dot{\boldsymbol{x}}} \\ \frac{\partial q_j}{\partial \boldsymbol{w}} \end{bmatrix}^T \begin{bmatrix} \frac{d\boldsymbol{u}}{ds_i} \\ \frac{d\dot{\boldsymbol{x}}}{ds_i} \\ \frac{d\boldsymbol{w}}{ds_i} \end{bmatrix} \tag{106}$$

Where the total complexity can be approximated as $\mathcal{O}(n_{eq}^2 n_{\boldsymbol{s}} + n_{\boldsymbol{q}} n_{eq} n_{\boldsymbol{s}})$

Adjoint approach Secondly, one could also first compute the derivatives of the optimization criteria and multiply with the Jacobian before substituting this into Equation (104):

$$\begin{bmatrix} \boldsymbol{a_u} \\ \boldsymbol{a_{\dot{x}}} \\ \boldsymbol{a_w} \end{bmatrix} = \boldsymbol{A}^{-T} \begin{bmatrix} \frac{\partial q_j}{\partial \boldsymbol{u}} \\ \frac{\partial q_j}{\partial \dot{\boldsymbol{x}}} \\ \frac{\partial q_j}{\partial \boldsymbol{w}} \end{bmatrix} \tag{107}$$

eq:firststep_adjoint

$$\frac{dq_j}{ds_i} = \frac{\partial q_j}{\partial s_i} - \begin{bmatrix} \boldsymbol{a_u} \\ \boldsymbol{a_{\dot{x}}} \\ \boldsymbol{a_w} \end{bmatrix}_j^T \begin{bmatrix} \frac{\partial \mathcal{S}_{gov}}{\partial s_i} \\ \frac{\partial \mathcal{D}_{gov}}{\partial s_i} \\ \frac{\partial \mathcal{F}_{gov}}{\partial s_i} \end{bmatrix} \tag{108}$$

Where the total complexity can be approximated as $\mathcal{O}(n_{eq}^2 n_{\boldsymbol{q}} + n_{\boldsymbol{q}} n_{eq} n_{\boldsymbol{s}})$

If one or the other approach is to be preferred depends in on the optimization setup, particularly the number of optimization criteria and the number of optimization variables. Looking at the orders above, one can conclude that if the number of abstract parameters $n_{\boldsymbol{s}}$ is smaller than the number of optimization criteria, the direct approach is more efficient, otherwise the adjoint approach is to be preferred. Additionally the on can argue, that the relevant term in the orders above is the one with n_{eq}^2 since it dominates the sum. Therefore, depending on whether n_s or n_q is bigger, the direct or the adjoint method is to be preferred.

7.1.1 Direct Sensitivity Analysis for the Euler equations

The A matrix for the direct approach in ALE formulation looks like

$$\boldsymbol{A} = \begin{bmatrix} \frac{\partial \mathcal{S}_{gov}}{\partial \boldsymbol{u}} & \frac{\partial \mathcal{S}_{gov}}{\partial \dot{\boldsymbol{x}}} & \frac{\partial \mathcal{S}_{gov}}{\partial \boldsymbol{w}} \\ \frac{\partial \mathcal{D}_{gov}}{\partial \boldsymbol{u}} & \frac{\partial \mathcal{D}_{gov}}{\partial \dot{\boldsymbol{x}}} & \boldsymbol{0} \\ \boldsymbol{0} & \frac{\partial \mathcal{F}_{gov}}{\partial \dot{\boldsymbol{x}}} & \frac{\partial \mathcal{F}_{gov}}{\partial \boldsymbol{w}} \end{bmatrix} = \begin{bmatrix} \mathbf{K} & \frac{\partial \boldsymbol{P}_T}{\partial \dot{\boldsymbol{x}}} & \frac{\partial \boldsymbol{P}_T}{\partial \boldsymbol{w}} \\ \begin{bmatrix} \mathbf{K}_{\Omega\Gamma}\mathbf{T}_u \\ \mathbf{T}_u \end{bmatrix} & \begin{bmatrix} \mathbf{K}_{\Omega\Omega} & \mathbf{0} \\ \mathbf{0} & \mathbf{I} \end{bmatrix} & \mathbf{0} \\ \mathbf{0} & \frac{\partial \mathbf{F}_2}{\partial \dot{\boldsymbol{x}}_\Omega} & \boldsymbol{H}_2 \end{bmatrix} \tag{109}$$

eq:Amatrix_ALE

Where, $\boldsymbol{H}_2$ is the Jacobian of the second order row flux. It shall be noted that constructing this Jacobian is not a trivial issue and takes up a lot of computational resources, especially for FV, as described in [3]. Investigation into whether this term can be approximated at first order were carried out in [9] and [10].
Furthermore, [11] considered replacing the two mesh motion related matrices $\frac{\partial \boldsymbol{P}_T}{\partial \dot{\boldsymbol{x}}}$ and $\frac{\partial \mathbf{F}_2}{\partial \dot{\boldsymbol{x}}_\Omega}$ by a transpirational boundary condition. The consequences of this approach are also investigated in [9] and [10].
This thesis, however, does not use any of this simplifications.
The derivation of the sensitivities, can be achieved in a staggered scheme, very similar to the one, described in **??TODO**. It consists of five steps.

1) Update the structural displacement sensitivity to a new time step BY differentiating equations (57) and (61) and applying an under relaxation, we can obtain

$$\frac{\mathrm{d}\boldsymbol{u}^{(n)}}{\mathrm{d}s_i} = (1-\theta)\frac{\mathrm{d}\boldsymbol{u}^{(n)}}{\mathrm{d}s_i} + \theta\frac{\mathrm{d}\bar{\boldsymbol{u}}}{\mathrm{d}s_i} \qquad \texttt{eq:underrelax\_structdisp} \tag{110}$$

where $\bar{\boldsymbol{u}}$ is obtained from:

$$\mathbf{K}\frac{\mathrm{d}\bar{\boldsymbol{u}}}{\mathrm{d}s_i} = \frac{\partial TODO}{\partial s_i} + \frac{\partial \mathbf{T}_u{}^{(n)}}{\partial s_i} - \frac{\partial \mathbf{K}}{\partial s_i}\boldsymbol{u} \qquad \texttt{eq:fictious\_structdisp} \tag{111}$$

2) Transfer sensitivity of structure motion to the interface

$$\frac{\mathrm{d}\boldsymbol{u}_T^{(n)}}{\mathrm{d}s_i} = \mathbf{T}_u\frac{\mathrm{d}\boldsymbol{u}^{(n)}}{\mathrm{d}s_i} \qquad \texttt{eq:interface\_projections} \tag{112}$$

3) Compute derivative of fluid mesh motion The fluid mesh motion is computed by solving the pseudo Dirichlet problem as described in [3]. By design, the fictions stiffness matrix $\bar{\mathbf{K}}$ does not depend on the abstract optimization variables $\boldsymbol{s}$

$$\bar{\mathbf{K}}_{\Omega\Omega}\frac{\mathrm{d}\dot{\boldsymbol{x}}_\Omega^{(n)}}{\mathrm{d}s_i} = -\bar{\mathbf{K}}_{\Omega\Gamma}\frac{\mathrm{d}\dot{\boldsymbol{x}}_\Gamma^{(n)}}{\mathrm{d}s_i} \qquad \texttt{eq:mms\_domain} \tag{113}$$

with

$$\frac{\mathrm{d}\dot{\boldsymbol{x}}_\Gamma^{(n)}}{\mathrm{d}s_i} = \frac{\mathrm{d}\dot{\boldsymbol{x}}_\Gamma^{(n)}}{\mathrm{d}s_i} \tag{114}$$

4) Compute the sensitivity of the fluid state variables The derivatives of the fluid state variables are computed by

$$\boldsymbol{H}_2\frac{\mathrm{d}\boldsymbol{w}^{(n+1)}}{\mathrm{d}s_i} = \frac{\partial \boldsymbol{F}_2}{\partial s_i} - \frac{\partial \boldsymbol{F}_2}{\partial \dot{\boldsymbol{x}}}\frac{\mathrm{d}\dot{\boldsymbol{x}}^{(n)}}{\mathrm{d}s_i} \tag{115}$$

5) Compute the sensitivity of the structure load vector The derivative of the fluid load with respect to the abstract variables can be computed by the third of Equations (105) with the definition of $\boldsymbol{A}$ as specified in (109).

$$\frac{\partial \boldsymbol{P}_F{}^{(n+1)}}{\partial s_i} = \frac{\partial \boldsymbol{P}_F{}^{(n+1)}}{\partial \dot{\boldsymbol{x}}} \frac{\mathrm{d}\dot{\boldsymbol{x}}^{(n)}}{\mathrm{d}s_i} + \frac{\partial \boldsymbol{P}_F{}^{(n+1)}}{\partial \boldsymbol{w}} \frac{\mathrm{d}\boldsymbol{w}^{(n)}}{\mathrm{d}s_i} \tag{116}$$

eq:deriv_floadBYabsvar

and compute project it onto the structure via

$$\frac{\partial \boldsymbol{P}_T{}^{(n+1)}}{\partial s_i} = \mathbf{T}_p \frac{\partial \boldsymbol{P}_F{}^{(n+1)}}{\partial s_i} \tag{117}$$

The convergence of the staggered algorithm can be monitored via

$$\left\| \mathbf{K} \frac{\mathrm{d}\bar{\boldsymbol{u}}^{(n+1)}}{\mathrm{d}s_i} - \frac{\partial TODO}{\partial s_i} - \frac{\partial \boldsymbol{P}_T{}^{(n+1)}}{\partial s_i} + \frac{\partial \mathbf{K}}{\partial s_i} \right\|_2 \leq \epsilon^{SA} \left\| \mathbf{K} \frac{\mathrm{d}\bar{\boldsymbol{u}}^{(0)}}{\mathrm{d}s_i} - \frac{\partial TODO}{\partial s_i} - \frac{\partial \boldsymbol{P}_T{}^{(0)}}{\partial s_i} + \frac{\partial \mathbf{K}}{\partial s_i} \right\|_2 \tag{118}$$

$$\left\| \boldsymbol{H}_2 \frac{\mathrm{d}\boldsymbol{w}^{(n+1)}}{\mathrm{d}s_i} + \frac{\partial \boldsymbol{F}_2}{\partial s_i} + \frac{\partial \boldsymbol{F}_2}{\partial \dot{\boldsymbol{x}}} \frac{\mathrm{d}\dot{\boldsymbol{x}}}{\mathrm{d}s_i}^{(n+1)} \right\|_2 \leq \epsilon^{SA} \left\| \boldsymbol{H}_2 \frac{\mathrm{d}\boldsymbol{w}^{(0)}}{\mathrm{d}s_i} + \frac{\partial \boldsymbol{F}_2}{\partial s_i} + \frac{\partial \boldsymbol{F}_2}{\partial \dot{\boldsymbol{x}}} \frac{\mathrm{d}\dot{\boldsymbol{x}}}{\mathrm{d}s_i}^{(0)} \right\|_2 \tag{119}$$

7.1.2 Adjoint Sensitivity Analysis for the Euler equations

The adjoint SA follows the same scheme as the direct one

Equation (107) can be written as:

$$\begin{bmatrix} \mathbf{K} & \begin{bmatrix} \frac{\partial \boldsymbol{P}_T}{\partial \dot{\boldsymbol{x}}_\Omega} & \frac{\partial \boldsymbol{P}_T}{\partial \dot{\boldsymbol{x}}_\Gamma} \end{bmatrix} & \frac{\partial \boldsymbol{P}_T}{\partial \boldsymbol{w}} \\ \begin{bmatrix} \mathbf{K}_{\Omega\Gamma}\mathbf{T}_u \\ \mathbf{T}_u \end{bmatrix} & \begin{bmatrix} \mathbf{K}_{\Omega\Omega} & \mathbf{0} \\ \mathbf{0} & \mathbf{I} \end{bmatrix} & \mathbf{0} \\ \mathbf{0} & \begin{bmatrix} \frac{\partial \mathbf{F}_2}{\partial \dot{\boldsymbol{x}}_\Omega} & \frac{\partial \mathbf{F}_2}{\partial \dot{\boldsymbol{x}}_\Gamma} \end{bmatrix} & \boldsymbol{H}_2 \end{bmatrix}^T \begin{bmatrix} \boldsymbol{a}_{\boldsymbol{u}} \\ \begin{bmatrix} \boldsymbol{a}_{\dot{\boldsymbol{x}}_\Omega} \\ \boldsymbol{a}_{\dot{\boldsymbol{x}}_\Gamma} \end{bmatrix} \\ \boldsymbol{a}_{\boldsymbol{w}} \end{bmatrix} = \begin{bmatrix} \frac{\partial q_j}{\partial \boldsymbol{u}} \\ \begin{bmatrix} \frac{\partial \boldsymbol{q}}{\partial \dot{\boldsymbol{x}}_\Omega} \\ \frac{\partial \boldsymbol{q}}{\partial \dot{\boldsymbol{x}}_\Gamma} \end{bmatrix} \\ \frac{\partial q_j}{\partial \boldsymbol{w}} \end{bmatrix} \tag{120}$$

eq:adjoint_equation

TODO check if the index j is really required here! A stated earlier, the matrices $\frac{\partial \boldsymbol{q}}{\partial \dot{\boldsymbol{x}}}$ and $\frac{\partial \boldsymbol{q}}{\partial \boldsymbol{w}}$ can be computed analytically. As for $\boldsymbol{H}_2$, we follow the methodology outlined in [7] for evaluating ans storing it efficiently as the product of flux operators. Again the staggered procedure for solving the adjoint state problem shares the same computational kernels with the partitioned aeroelastic scheme described in [3]

1) Update the adjoint structure displacement to the new time step

$$\boldsymbol{a_u}^{(n+1)} = (1-\theta)\boldsymbol{a_u}^{(n)} + \theta\bar{\boldsymbol{a_u}}^{(n+1)} \tag{121}$$

$$\tag{122}$$

where $\bar{\boldsymbol{a_u}}^{(n+1)}$ is obtained from

$$\mathbf{K}\bar{\boldsymbol{a_u}}^{(n+1)} = \frac{\partial \boldsymbol{q}}{\partial \boldsymbol{u}} - \mathbf{K}_{\Omega\Gamma}\mathbf{T}_u\boldsymbol{a_{x\Omega}}^{(n)} + \mathbf{T}_u\boldsymbol{a_{x\Gamma}}^{(n)} \tag{123}$$

TODO derive this equation

2) Compute the adjoint fluid state by solving

$$\boldsymbol{H}_2{}^T\boldsymbol{a_w}^{(n+1)} = \frac{\partial \dot{\boldsymbol{x}}}{\partial \boldsymbol{w}} + \frac{\partial \boldsymbol{P}_T}{\partial \boldsymbol{w}^T}\boldsymbol{a_u}^{(n+1)} \tag{124}$$

TODO derive this equation Again, $\dfrac{\partial \boldsymbol{q}}{\partial \boldsymbol{w}}$ is computed analytically from the relations defined in the design and aeroelastic model.

3) Compute adjoint mesh motion in domain and on the interface

$$\bar{\mathbf{K}}_{\Omega\Omega}\boldsymbol{a_{x\Omega}}^{(n+1)} = \frac{\partial \boldsymbol{q}}{\partial \dot{\boldsymbol{x}}_\Omega} - \frac{\partial \boldsymbol{P}_T}{\partial \dot{\boldsymbol{x}}_\Omega}\boldsymbol{a_u}^{(n+1)} - \frac{\partial \mathbf{F}_1{}^T}{\partial \dot{\boldsymbol{x}}_\Omega}\boldsymbol{a_x}^{(n+1)} \text{ in } \Omega \tag{125}$$

TODO check equations And the adjoint mesh motion on the interface is computed as $\boldsymbol{a_{x\Gamma}}^{(n+1)}$

$$\boldsymbol{a_{x\Gamma}}^{(n+1)} = \frac{\partial \boldsymbol{q}}{\partial \dot{\boldsymbol{x}}_{Gamma}} + \frac{\partial \boldsymbol{P}_T}{\partial \dot{\boldsymbol{x}}_\Gamma}\boldsymbol{a_u}^{(n+1)} - \frac{\partial \mathbf{F}_2}{\partial \dot{\boldsymbol{x}})_\Gamma}{}^T \text{ on } \Gamma \tag{126}$$

where $\dfrac{\partial \boldsymbol{q}}{\partial \boldsymbol{w}}$ is computed analytically.

The convergence of the staggered adjoint optimization algorithm can be monitored via

$$\left\| \boldsymbol{R_q} - \boldsymbol{A}^T\boldsymbol{a}^{(n+1)} \right\| \leq \epsilon^{SA} \left\| \boldsymbol{R_q} \right\| \tag{127}$$

8 Fiver

It was already outlined in Section 2, that using an Eulerian approach int the context of an aeroelastic simulation leads to a so-called embedded formulation, where the interface of the structure mesh no longer coincides with the fluid mesh. This was appealing, since it allowed for the usage of fixed meshes and an Eulerian formulation, on the other hand as explained in Section **??**, an error of the order $\mathcal{O}(\frac{h}{2})$ is introduced. A possible solution to recover second order convergence rate is quickly described in section **TODO**.

8.1 Setup

In this thesis, we consider embedded structure interfaces only. Whether the structure is deformable or rigid does not really make a difference for the subsequent considerations.
The basic setup is depicted in Figure 8.
Several issues have to be addresses in an embedded framework. Firstly, the interface may move during the simulation. In fact, large deformations of the structure have been on on the primary aspects for the development of an embedded framework in the first place. The question thus becomes how to track the interface during the simulation. This is addressed in section 8.2.
Secondly, the evaluation of the inviscid (129) and viscous (133) term becomes cumbersome for cells that are being intersected. We address this issue separate for the inviscid and the viscous term in sections 8.3 and 8.4.
Finally, in an FSI simulation we are typically interested in integral quantities over the structure surface, e.g. the lift and drag values of an airfoil. We now have several possibilities to define the structure surface to perform integration on in an embedded simulation. This issues will is discussed in section 8.5.

8.2 Level-set method

The issue of interface tracking is extensively discussed in **CITEWangGretarsson2012** and TODO.

Since the interface in an embedded stimulation typically moves, an appropriate interface tracking approach is required.
For FIVER, the popular level set method [13] was chosen.

The level set approach is characterized by the following equation:

$$\frac{\phi}{t} + \boldsymbol{v} \cdot \nabla\phi = 0 \tag{128}$$ eq:level_set

where ϕ is a function designed to track the material interface. Particularly, ϕ is initialized such that that the interface is characterized by $\phi = 0$. The interface can then be tracked via a simple time integration of equation (128). Details of this approach, which was developed for computer visualization purposes, can be found in [13].

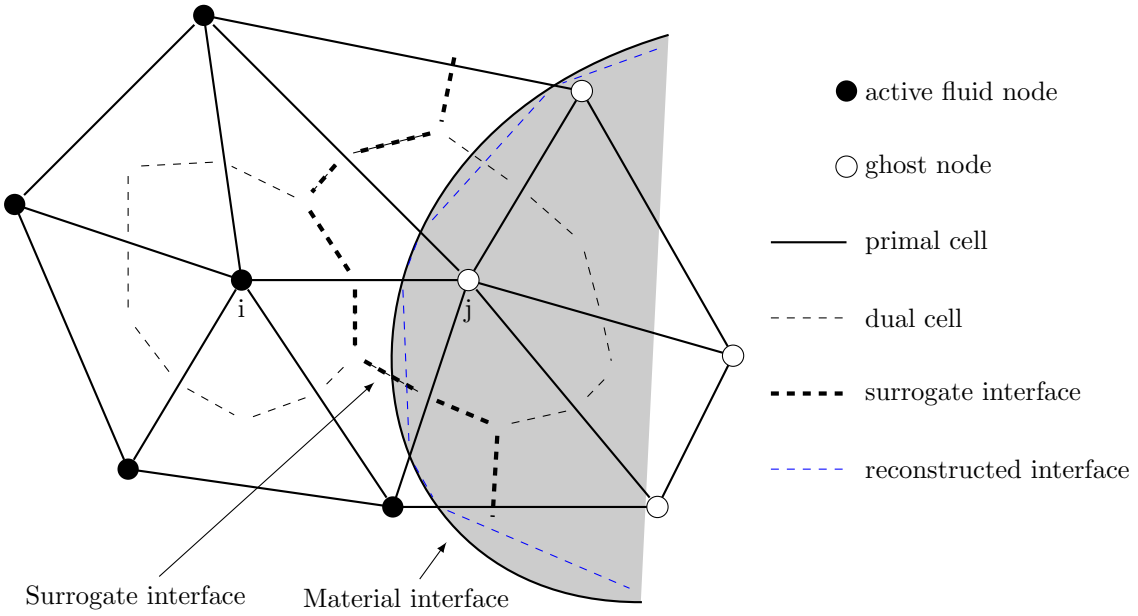

Figure 8: Sketch of an embedded simulation setup. The primal grid is intersected by a material interface. In FIVER, the material interface is replaced by a surrogate interface that is created by connecting the dual-grid interfaces closest to the embedded surface. By connecting the intersection points of the embedded surface with the primal grid, we can also create a so-called, reconstructed surface that is particularly useful for the calculation of forces on the surface.

TODO

8.3 Evaluation of the inviscid term at the interface

For this section as well as for section 8.4 we consider Figure 8.
A question, that arrises when lookin at equation (40) is how to evaluate those terms for node i, where some of the vertices in $\kappa(i)$ are inactive ghost nodes.
We will answer this question for the inviscid term in this subsections and look at the viscous term in the subsequent one.

First, we notice that we can split the summation as follows

$$\sum_{j\in\kappa(i)} \boldsymbol{\phi}_{ij}(\boldsymbol{w}_i, \boldsymbol{w}_j, \boldsymbol{\nu}_{ij}) = \sum_{j\in\kappa(i)^a} \boldsymbol{\phi}_{ij}(\boldsymbol{w}_i, \boldsymbol{w}_j, \boldsymbol{\nu}_{ij}) + \sum_{j\in\kappa(i)\setminus\kappa(i)^a} \boldsymbol{\phi}_{ij}(\boldsymbol{w}_i, \boldsymbol{w}_*, \boldsymbol{\nu}_{ij}) \tag{129}$$

eq:fiver_inviscid_split

where $\boldsymbol{w}_*$ is the fluid state at the auxiliary intersection between edge ij and the auxiliary interface. To obtain $\boldsymbol{w}_8$ a one-sided Riemann problem is defined

$$\frac{\partial \tilde{\boldsymbol{w}}}{\partial t} = \frac{\partial \mathcal{F}}{\partial s}(\tilde{\boldsymbol{w}}) = \boldsymbol{0} \tag{130}$$

where s is the local abscissa along the direction ij, that has its origin in M_{ij}.
The one sided Riemann problem can then be initialized with

$$\tilde{\boldsymbol{w}}_L = \begin{bmatrix} \rho_i & \boldsymbol{v}_i & p_i \end{bmatrix} \tag{131}$$

The exact solution of the one-sided, one-dimensional Riemann problem contains a constatn (in time) state at the fluid-structure interface which is denoted here by

$$\boldsymbol{w}_* = \begin{bmatrix} \rho_* & \boldsymbol{v}_* & p_* \end{bmatrix} \tag{132}$$

which can then be used in equation (129)

8.4 Evaluation of the viscous terms at the interface

If one wants to keep the FE-like evaluation of the second term, (40) can be splitted as

$$\sum_{T_i \in \lambda(i)} \int_{T_i} \mathbb{K} \nabla \boldsymbol{w} \nabla \phi_i dx = \sum_{T_i \in (\lambda(i^a))} \int_{T_i} \mathbb{K} \nabla \boldsymbol{w} \nabla \phi_i dx + \sum_{T_i \in (\lambda(i) \setminus \lambda(i^a))} \int_{T_i} \mathbb{K} \nabla \boldsymbol{w}^R \nabla \phi_i dx = \tag{133}$$

eq:fiver_viscous_split

where $\lambda(i^a)$ is the set of triangles that can be build from the active nodes around node i and $\lambda(i) \setminus \lambda(i^a)$ are all the triangles where at least one node is inactive(ghost).

The only difficulty now becomes the evaluation of the last term, meaning the integration over cutted elements, where at least on node is inactive, and thus does not have a fluid state solution.
We did not have that problem for the inviscid term of equation (40), since a FV approximation was chosen, and therefore we could construct a flux at the interface thanks to the piston problem. No inactive node had to be considered.
For the viscous part, however, we want to keep the FE like formulations described in 3.3 to avoid re-writing large portions of the code. If a triangle is cut by the interface, one or two nodes will therefor be labeled inactive, and be denoted as ghost-nodes. Clearly, the fluid state vector at this ghost nodes is not defined. The question thus becomes how to evaluate this terms (last part in equation (133)).

The approach we take, that is also outlined in **TODO ask for reference** is to reconstruct a pseudo fluid-state at the ghost points, such that the boundary conditions at the wall are full-filled.

8.4.1 Reconstruction of the fluid-state at ghost-nodes

TODO ask Farhat if this is really how it is done To explain the reconstruction at the ghost nodes, it again helps to consider Figure 8.
We also notice that the viscous flux, as defined in Equation 19, only depends on the fluid velocity and the temperature. Reconstruction of the velocity at the ghost

node is straight forward. Assuming a linear interpolation inside the elements, the velocity at node i is reconstructed such, that the stick condition is fulfilled at the interface.
As far as the reconstruction of the temperature is concerned, two different cases have to be considered: adiabatic walls and isothermal walls.
For an adiabatic wall, the temperature gradient at the wall is zeros, which can be achieved by setting the temperature of the ghost note equal to that of node i. An isothermal wall boundary condition enforces a certain, constant temperature at the wall. Similar to the velocity boundary condition, this can be achieved by finding an appropriate ghost point value such that the condition is enforces.
Figure 8 also reveals that there is no unique solution for the ghost point value. Multiple active node connect to the ghost node and the above described relations can be formulated for every one of them. FIVER therefore solves a least square system to chose an appropriate value.
The elegance of this approach is that once the ghost point state have been found, the evaluation of the viscous contribution can be done with the standard code routines. No adaption is required to make them work in the embedded framework.

8.5 Evaluation of forces

Another issue that arises for embedded simulations is the appropraite evaluation of the forces on an embedded interface. This is especially important if the embedded framework is used in an FSI setup to get an approriate resultant on the structure. Sensitivity Analysis is another application, where approriate evaluation of Lift and Drag integrals are crucial.
This problem as been analyzed in **REF REF** MOst importantly, the qeustion becomes whether to evaluate the pressure integral **REF** over the ausivilary control volume interface **Ref** or over the so called reconstructed interface, which can be obtained by creating ausiliary surfaces inside the intersected elements through the knowledge ablout intersection points at the edges.

9 Derivative of the Numerical flux with respect to the fluid state variables

This section is denoted to a thorough derivation of the derivative $\frac{\partial \boldsymbol{\phi}}{\partial \boldsymbol{w}_i}$.

First, we recall the definition of the numerical flux as

$$\boldsymbol{\phi}(\mathbf{w}_i, \mathbf{w}_j, \boldsymbol{n}_{ij}) = \frac{1}{2}\left[\mathcal{F}(\mathbf{w}_i)\cdot\boldsymbol{n}_{ij} + \mathcal{F}(\mathbf{w}_i)\cdot\boldsymbol{n}_{ij}\right] - \frac{1}{2}|\boldsymbol{A}_{\text{Roe}}(\mathbf{w}_i, \mathbf{w}_j, \boldsymbol{n}_{ij})|(\mathbf{w}_j - \mathbf{w}_i) \tag{134}$$

eq:roe_flux

Similar to the MUSCL procedure we transform the fluid state vector to primitive form

$$\boldsymbol{w} = \begin{pmatrix} \rho \\ \rho\boldsymbol{v} \\ E \end{pmatrix} \overset{\cup}{\mapsto} \tilde{\boldsymbol{w}} = \begin{pmatrix} \rho \\ \boldsymbol{v} \\ p \end{pmatrix} \tag{135}$$

Of course, this transformation involves the EOS of the fluid. We will use $\tilde{(\cdot)}$ from now on top mark any quantity as based on/formulated in primitive variables.
The primitive state vector is also much more appealing when it comes to the implementation of boundary conditions, since the solution variables are separated there.
Next we recall the conservative form of the Euler equations, which was presented in section 2.2.4 as

$$\frac{\partial \boldsymbol{w}}{\partial t} + \nabla\cdot\mathcal{F}\boldsymbol{w} = \mathbf{0} \tag{136}$$

eq:t1

Where the convective flux matrix $\mathcal{F}$ is provided in equation (16), and can be written as

$$\mathcal{F}(\boldsymbol{w}) = \begin{pmatrix} \mathcal{F}_x(\boldsymbol{w}) & \mathcal{F}_x(\boldsymbol{w}) & \mathcal{F}_x(\boldsymbol{w}) \end{pmatrix} \tag{137}$$

Therefore, applying the Nabla operator in Equation (136) gives

$$\frac{\partial \boldsymbol{w}}{\partial t} + \underbrace{\frac{\partial \mathcal{F}_x(\boldsymbol{w})}{\partial \boldsymbol{w}}}_{\boldsymbol{A}}\frac{\partial \boldsymbol{w}}{\partial x} + \underbrace{\frac{\partial \mathcal{F}_y(\boldsymbol{w})}{\partial \boldsymbol{w}}}_{\boldsymbol{B}}\frac{\partial \boldsymbol{w}}{\partial y} + \underbrace{\frac{\partial \mathcal{F}_z(\boldsymbol{w})}{\partial \boldsymbol{w}}}_{\boldsymbol{C}}\frac{\partial \boldsymbol{w}}{\partial z} = \mathbf{0} \tag{138}$$

eq:euler_conservative_splitted

where the matrices $\boldsymbol{A}$,$\boldsymbol{B}$ and $\boldsymbol{C}$ are called the *flux Jacobians*.

In Section 6, we have derived that for any sensitivity calculation, the derivative of the flux matrix with respect to the fluid state vector $\frac{\partial \mathbf{F}}{\partial \boldsymbol{w}}$ is required.

We have derived in Section 3.3 that at an interior vertex point of the fluid mesh, we have

$$[\mathbf{F}(\mathbf{w},\mathbf{x},\dot{\mathbf{x}})]_i = \sum_{j\in\kappa(i)} mes(\partial C_{ij})\boldsymbol{\phi}(\mathbf{w}_i,\mathbf{w}_j,\boldsymbol{n}_{ij}) \tag{139}$$

eq:convectiveterm _approximation2

Since an equilibrium point is considered, $\dot{\mathbf{x}} = \mathbf{0}$ and is neglected in the following derivations.

In equation (38) we have introduced $\boldsymbol{\phi}$ as the numerical flux function. In this thesis, we consider the popular Roe flux, which is defined as given in equation (134).

Let us remind, that $\mathbf{w}_i$ is the flux vector at vertex i, $\kappa(i)$ is the set of vertices connected to vertex i by an edge, C_i is the control volume of the dual cell centered at vertex i and ∂C_{ij} is the segment of the boundary that intersects edge (ij) and $\boldsymbol{\nu}_{ij}$ is the outward-facing weighted normal to ∂C_{ij}

From Equation (139) it is obvious that when looking for the derivative $\dfrac{\partial \mathbf{F}}{\partial \mathbf{w}}$, the derivative of the numerical flux with respect to the fluid state vector $\dfrac{\partial \boldsymbol{\phi}}{\partial \mathbf{w}}$ is required.

To make things easier we will in the following derive the primitive version of that quantity $\dfrac{\partial \tilde{\boldsymbol{\phi}}}{\partial \tilde{\mathbf{w}}}$

The primitive version of the numerical Roe flux can be expressed as

$$\tilde{\mathcal{F}}(\tilde{\mathbf{w}}_i,\tilde{\mathbf{w}}_j,\boldsymbol{n}_{ij}) = \frac{1}{2}\left(\tilde{\mathcal{F}}(\tilde{\mathbf{w}}_i)\cdot\boldsymbol{n}_{ij} + \tilde{\mathcal{F}}(\tilde{\mathbf{w}}_i)\cdot\boldsymbol{n}_{ij}\right) - \frac{1}{2}\boldsymbol{P}^{-1}(\sim)|\boldsymbol{\Lambda}(\sim)|\boldsymbol{P}(\sim)(\tilde{\mathbf{w}}_j - \tilde{\mathbf{w}}_i) \tag{140}$$

$$\tag{141}$$

TODO where did the absolute value go? TODO what is M where, for ease of notation

$$\boldsymbol{P}^{-1}(\sim) = \boldsymbol{P}^{-1}\left(\boldsymbol{M}(\sim),\boldsymbol{n}_{ij}\right) \tag{142}$$

$$\boldsymbol{M}(\sim) = \boldsymbol{M}\left(\tilde{\boldsymbol{w}}_i,\tilde{\boldsymbol{w}}_j\right) \tag{143}$$

$$\boldsymbol{\Lambda}(\sim) = \boldsymbol{\Lambda}\left(\boldsymbol{M}(\sim),\boldsymbol{n}_{ij}\right) \tag{144}$$

$$\boldsymbol{P}(\sim) = \boldsymbol{P}\left(\boldsymbol{M}(\sim),\boldsymbol{n}_{ij}\right) \tag{145}$$

$$\tag{146}$$

Here, $\boldsymbol{M}(\tilde{\boldsymbol{w}}_i,\tilde{\boldsymbol{w}}_j)$ is the averaging function associated with the roe flux. It can be written as

$$\boldsymbol{M}(\tilde{\boldsymbol{w}}_i,\tilde{\boldsymbol{w}}_j) = \frac{1}{\sqrt{\rho_i}+\sqrt{\rho_j}}\left(\sqrt{\rho_i}\begin{bmatrix}\rho_i\\ \boldsymbol{v}_i\\ \mathsf{H}_i\end{bmatrix} + \sqrt{\rho_j}\begin{bmatrix}\rho_j\\ \boldsymbol{v}_j\\ \mathsf{H}_j\end{bmatrix}\right) \tag{147}$$

The Jacobi matrix in primitive form can be written as
TODO notation

$$\tilde{\mathcal{A}} = \frac{\partial(\tilde{\mathcal{F}} \cdot \boldsymbol{n})}{\partial \tilde{\boldsymbol{w}}} \tag{148}$$

$$= \begin{bmatrix} \boldsymbol{v}\cdot\boldsymbol{n} & \rho n_x & \rho n_y & \rho n_z & 0 \\ v_1(\boldsymbol{v}\cdot\boldsymbol{n}) & \rho(\boldsymbol{v}\cdot\boldsymbol{n}) + \rho v_1 n_1 & \rho v_1 n_2 & \rho v_1 n_3 & n_1 \\ v_2(\boldsymbol{v}\cdot\boldsymbol{n}) & \rho v_2 n_1 & \rho(\boldsymbol{v}\cdot\boldsymbol{n}) + \rho v_2 n_2 & \rho v_2 n_3 & n_2 \\ v_3(\boldsymbol{v}\cdot\boldsymbol{n}) & \rho v_3 n_1 & \rho v_3 n_2 & \rho(\boldsymbol{v}\cdot\boldsymbol{n}) + \rho v_3 n_3 & n_2 \\ A_{51} & A_{52} & A_{53} & A_{54} & A_{55} \end{bmatrix}$$

$$\begin{aligned} \mathcal{A}_{51} &= H\ (\boldsymbol{v}\cdot\boldsymbol{n}) - \rho\boldsymbol{v}\cdot\boldsymbol{n}\frac{\gamma p}{\rho(\gamma)} \\ \mathcal{A}_{52} &= \rho\boldsymbol{v}\cdot\boldsymbol{n}v_1 + \rho H n_1 \\ \mathcal{A}_{53} &= \rho\boldsymbol{v}\cdot\boldsymbol{n}v_2 + \rho H n_2 \\ \mathcal{A}_{54} &= \rho\boldsymbol{v}\cdot\boldsymbol{n}v_3 + \rho H n_3 \\ \mathcal{A}_{55} &= \rho\boldsymbol{v}\cdot\boldsymbol{n}\frac{\gamma}{\rho(\gamma-1)} \end{aligned} \tag{149}$$

For this Jacobian, one can now symbolically derive an eigenvalue decomposition, such that **TODO notation**

$$\tilde{\mathcal{H}} = \boldsymbol{P}^{-1}\boldsymbol{\Lambda}\boldsymbol{P} \tag{150}$$

The total specific enthalpy for a perfect gas is given as

$$\mathsf{H} = \frac{\gamma p}{\rho(\gamma-1)} + \frac{1}{2}\boldsymbol{v}^T\boldsymbol{v} \tag{151}$$

where we note the following derivatives

$$\frac{\partial \mathsf{H}}{\partial \rho} = -\frac{\gamma p}{\rho^2(\gamma-1)} \qquad \frac{\partial \mathsf{H}}{\partial v_i} = v_i \qquad \frac{\partial \mathsf{H}}{\partial p} = \frac{\gamma}{\rho(\gamma-1)} \tag{152}$$

Therefore, the derivative of the averaging function with respect to the primitive

fluid state vector can be calculated as

$$\frac{\partial \boldsymbol{M}(\sim)}{\partial \rho_i} = \frac{1}{2\sqrt{\rho_i}(\sqrt{\rho_i}+\sqrt{\rho_j})}\left(-\boldsymbol{M}(\sim) + \begin{bmatrix} 3\rho_i & 2\sqrt{\rho_i}\boldsymbol{v}_i & 2\mathsf{H}_i - 2\rho_i\dfrac{\gamma p}{\rho^2(\gamma-1)} \end{bmatrix}^T\right)$$

$$\frac{\partial \boldsymbol{M}(\sim)}{\partial v_i} = \frac{1}{(\sqrt{\rho_i}+\sqrt{\rho_j})}\sqrt{\rho_i}\begin{bmatrix} 0 & \boldsymbol{e}_i{}^T & v_i \end{bmatrix}^T$$

$$\frac{\partial \boldsymbol{M}(\sim)}{\partial p_i} = \frac{1}{(\sqrt{\rho_i}+\sqrt{\rho_j})}\sqrt{\rho_i}\begin{bmatrix} 0 & \boldsymbol{0}^T & \dfrac{\gamma}{\rho(\gamma-1)} \end{bmatrix}^T$$

$$\frac{\partial \boldsymbol{M}(\sim)}{\partial \tilde{\boldsymbol{w}}_i} = \begin{bmatrix} 3\rho_i - \dfrac{\sqrt{\rho_i}\rho_i + \sqrt{\rho_j}\rho_j}{\sqrt{\rho_i}+\sqrt{\rho_j}} & 0 & 0 & 0 & 0 \\ v_{1i} - \dfrac{\sqrt{\rho_i}v_{1i} + \sqrt{\rho_j}v_{1j}}{\sqrt{\rho_i}+\sqrt{\rho_j}} & 2\rho_i & 0 & 0 & 0 \\ v_{2i} - \dfrac{\sqrt{\rho_i}v_{2i} + \sqrt{\rho_j}v_{2j}}{\sqrt{\rho_i}+\sqrt{\rho_j}} & 0 & 2\rho_i & 0 & 0 \\ v_{3i} - \dfrac{\sqrt{\rho_i}v_{3i} + \sqrt{\rho_j}v_{3j}}{\sqrt{\rho_i}+\sqrt{\rho_j}} & 0 & 0 & 2\rho_i & 0 \\ \dfrac{\boldsymbol{v}^T\boldsymbol{v}}{2} - \dfrac{\gamma p}{\rho(\gamma-1)} - \dfrac{\sqrt{\rho_i}\mathsf{H}_i + \sqrt{\rho_j}\mathsf{H}_j}{\sqrt{\rho_i}+\sqrt{\rho_j}} & 2\rho_i v_{1i} & 2\rho_i v_{1i} & 2\rho_i v_{1i} & \dfrac{2\gamma}{\gamma-1} \end{bmatrix} \tag{153}$$

The matrix $\boldsymbol{P}$ can be written as

$$\boldsymbol{P} = \begin{bmatrix} \left(\boldsymbol{n} - \frac{(\gamma-1)\boldsymbol{v}^T\boldsymbol{v}}{2c^2}\boldsymbol{n} + \boldsymbol{n}\times\boldsymbol{v}\right)\cdot\boldsymbol{e}_1 & n_1(\gamma-1)\frac{v_1}{c^2} & n_1(\gamma-1)\frac{v_2}{c^2}+n_3 & n_1(\gamma-1)\frac{v_3}{c^2}-n_2 & -n_1\frac{\gamma-1}{c^2} \\ \left(\boldsymbol{n} - \frac{(\gamma-1)\boldsymbol{v}^T\boldsymbol{v}}{2c^2}\boldsymbol{n} + \boldsymbol{n}\times\boldsymbol{v}\right)\cdot\boldsymbol{e}_2 & n_2(\gamma-1)\frac{v_1}{c^2}-n_3 & n_2(\gamma-1)\frac{v_2}{c^2} & n_2(\gamma-1)\frac{v_3}{c^2}+n_1 & -n_2\frac{\gamma-1}{c^2} \\ \left(\boldsymbol{n} - \frac{(\gamma-1)\boldsymbol{v}^T\boldsymbol{v}}{2c^2}\boldsymbol{n} + \boldsymbol{n}\times\boldsymbol{v}\right)\cdot\boldsymbol{e}_3 & n_3(\gamma-1)\frac{v_1}{c^2}+n_2 & n_3(\gamma-1)\frac{v_2}{c^2}-n_1 & n_3(\gamma-1)\frac{v_3}{c^2} & -n_2\frac{\gamma-1}{c^2} \\ (\gamma-1)\frac{\boldsymbol{v}^T\boldsymbol{v}}{c^2} - c\boldsymbol{v}\cdot\boldsymbol{n} & -(\gamma-1)v_1 + cn_1 & -(\gamma-1)v_2 + cn_2 & -(\gamma-1)v_3 + cn_3 & \gamma-1 \\ (\gamma-1)\frac{\boldsymbol{v}^T\boldsymbol{v}}{c^2} - c\boldsymbol{v}\cdot\boldsymbol{n} & -(\gamma-1)v_1 - cn_1 & -(\gamma-1)v_2 - cn_2 & -(\gamma-1)v_3 - cn_3 & \gamma-1 \end{bmatrix} \tag{154}$$

where c is the speed of sound given by $c = \sqrt{\dfrac{\gamma p}{\rho}}$

The matrix $\boldsymbol{\Lambda}$ derives to

$$\boldsymbol{\Lambda} = diag([\boldsymbol{v}\cdot\boldsymbol{n}, \boldsymbol{v}\cdot\boldsymbol{n}, \boldsymbol{v}\cdot\boldsymbol{n}, \boldsymbol{v}\cdot\boldsymbol{n}+c, \boldsymbol{v}\cdot\boldsymbol{n}-c)]) \tag{155}$$

$$\frac{\partial \boldsymbol{P}^{-1}}{\partial \tilde{\boldsymbol{w}}}(\tilde{\boldsymbol{w}}, \boldsymbol{n})\cdot b = \begin{bmatrix} \dfrac{\partial r_1}{\partial \tilde{\boldsymbol{w}}}(\tilde{\boldsymbol{w}}, \boldsymbol{n})\cdot b & \dfrac{\partial r_2}{\partial \tilde{\boldsymbol{w}}}(\tilde{\boldsymbol{w}}, \boldsymbol{n})\cdot b & \dfrac{\partial r_3}{\partial \tilde{\boldsymbol{w}}}(\tilde{\boldsymbol{w}}, \boldsymbol{n})\cdot b & \dfrac{\partial r_4}{\partial \tilde{\boldsymbol{w}}}(\tilde{\boldsymbol{w}}, \boldsymbol{n})\cdot b & \dfrac{\partial r_5}{\partial \tilde{\boldsymbol{w}}}(\tilde{\boldsymbol{w}}, \boldsymbol{n})\cdot b \end{bmatrix} \tag{156}$$

$$\frac{\partial r_1}{\partial \tilde{\boldsymbol{w}}}(\tilde{\boldsymbol{w}}, \boldsymbol{n}) = \begin{bmatrix} 0 & 0 & 0 & 0 & 0 \\ 0 & \boldsymbol{n}_x & 0 & 0 & 0 \\ 0 & 0 & \boldsymbol{n}_x & 0 & 0 \\ 0 & 0 & 0 & \boldsymbol{n}_x & 0 \\ 0 & v_1\boldsymbol{n}_x & v_2 n_1 + n_3 & v_3 n_1 - n_2 & 0 \end{bmatrix} \tag{157}$$

$$\frac{\partial r_2}{\partial \tilde{\boldsymbol{w}}}(\tilde{\boldsymbol{w}}, \boldsymbol{n}) = \begin{bmatrix} 0 & 0 & 0 & 0 & 0 \\ 0 & \boldsymbol{n}_y & 0 & 0 & 0 \\ 0 & 0 & \boldsymbol{n}_y & 0 & 0 \\ 0 & 0 & 0 & \boldsymbol{n}_y & 0 \\ 0 & v_1 n_2 - n_3 & v_2 n_2 & v_3 n_2 - n_1 & 0 \end{bmatrix} \tag{158}$$

$$\frac{\partial r_3}{\partial \tilde{\boldsymbol{w}}}(\tilde{\boldsymbol{w}}, \boldsymbol{n}) = \begin{bmatrix} 0 & 0 & 0 & 0 & 0 \\ 0 & \boldsymbol{n}_z & 0 & 0 & 0 \\ 0 & 0 & \boldsymbol{n}_z & 0 & 0 \\ 0 & 0 & 0 & \boldsymbol{n}_z & 0 \\ 0 & v_1 n_3 + n_2 & v_2 n_3 - n_1 & v_3 n_3 & 0 \end{bmatrix} \tag{159}$$

$$\frac{\partial r_4}{\partial \tilde{\boldsymbol{w}}}(\tilde{\boldsymbol{w}}, \boldsymbol{n}) = \begin{bmatrix} \frac{1}{2\gamma p} & 0 & 0 & 0 & -\frac{\rho}{2\gamma p^2} \\ \frac{v_1}{2\rho c^2} + \frac{n_1}{4\rho c} & \frac{1}{2c^2} & 0 & 0 & -\frac{v_1}{2pc^2} - \frac{n_1}{4pc} \\ \frac{v_2}{2\rho c^2} + \frac{n_2}{4\rho c} & 0 & \frac{1}{2c^2} & 0 & -\frac{v_2}{2pc^2} - \frac{n_2}{4pc} \\ \frac{v_3}{2\rho c^2} + \frac{n_3}{4\rho c} & 0 & 0 & \frac{1}{2c^2} & -\frac{v_3}{2pc^2} - \frac{n_3}{4pc} \\ \frac{1}{2\gamma} + \frac{\boldsymbol{v}\cdot\boldsymbol{n}}{4\rho c} & \frac{n_1}{2c} & \frac{n_2}{2c} & \frac{n_3}{2c} & -\frac{\boldsymbol{v}\cdot\boldsymbol{n}}{4pc} \end{bmatrix} \tag{160}$$

$$\frac{\partial r_5}{\partial \tilde{\boldsymbol{w}}}(\tilde{\boldsymbol{w}}, \boldsymbol{n}) = \begin{bmatrix} \frac{1}{2\gamma p} & 0 & 0 & 0 & -\frac{\rho}{2\gamma p^2} \\ \frac{v_1}{2\rho c^2} - \frac{n_1}{4\rho c} & \frac{1}{2c^2} & 0 & 0 & -\frac{v_1}{2pc^2} + \frac{n_1}{4pc} \\ \frac{v_2}{2\rho c^2} - \frac{n_2}{4\rho c} & 0 & \frac{1}{2c^2} & 0 & -\frac{v_2}{2pc^2} + \frac{n_2}{4pc} \\ \frac{v_3}{2\rho c^2} - \frac{n_3}{4\rho c} & 0 & 0 & \frac{1}{2c^2} & -\frac{v_3}{2pc^2} + \frac{n_3}{4pc} \\ \frac{1}{2\gamma} - \frac{\boldsymbol{v}\cdot\boldsymbol{n}}{4\rho c} & -\frac{n_1}{2c} & -\frac{n_2}{2c} & -\frac{n_3}{2c} & \frac{\boldsymbol{v}\cdot\boldsymbol{n}}{4pc} \end{bmatrix} \tag{161}$$

Due to its shape, the derivation of $\boldsymbol{\Lambda}$ can be simplified to a differentiation of the eigenvalues λ_i.

$$\frac{\partial \lambda_1}{\partial \tilde{\boldsymbol{w}}}(\tilde{\boldsymbol{w}}, \boldsymbol{n}) = \frac{\partial \lambda_2}{\partial \tilde{\boldsymbol{w}}}(\tilde{\boldsymbol{w}}, \boldsymbol{n}) = \frac{\partial \lambda_3}{\partial \tilde{\boldsymbol{w}}}(\tilde{\boldsymbol{w}}, \boldsymbol{n}) = \begin{bmatrix} 0 & \boldsymbol{n}^T & 0 \end{bmatrix}^T \tag{162}$$

$$\frac{\partial \lambda_4}{\partial \tilde{\boldsymbol{w}}}(\tilde{\boldsymbol{w}}, \boldsymbol{n}) = \begin{bmatrix} -\frac{c}{2\rho} & \boldsymbol{n}^T & \frac{c}{2p} \end{bmatrix}^T \tag{163}$$

$$\frac{\partial \lambda_5}{\partial \tilde{\boldsymbol{w}}}(\tilde{\boldsymbol{w}}, \boldsymbol{n}) = \begin{bmatrix} \frac{c}{2\rho} & \boldsymbol{n}^T & -\frac{c}{2p} \end{bmatrix}^T \tag{164}$$

$$\tag{165}$$

$$\frac{\partial \boldsymbol{P}}{\partial \tilde{\boldsymbol{w}}}(\tilde{\boldsymbol{w}}, \boldsymbol{n}) \cdot b = \begin{bmatrix} \frac{\partial l_1}{\partial \tilde{\boldsymbol{w}}}^T(\tilde{\boldsymbol{w}}, \boldsymbol{n}) \cdot b \\ \frac{\partial l_2}{\partial \tilde{\boldsymbol{w}}}^T(\tilde{\boldsymbol{w}}, \boldsymbol{n}) \cdot b \\ \frac{\partial l_3}{\partial \tilde{\boldsymbol{w}}}^T(\tilde{\boldsymbol{w}}, \boldsymbol{n}) \cdot b \\ \frac{\partial l_4}{\partial \tilde{\boldsymbol{w}}}^T(\tilde{\boldsymbol{w}}, \boldsymbol{n}) \cdot b \\ \frac{\partial l_5}{\partial \tilde{\boldsymbol{w}}}^T(\tilde{\boldsymbol{w}}, \boldsymbol{n}) \cdot b \end{bmatrix} \tag{166}$$

$$\frac{\partial l_1}{\partial \tilde{\boldsymbol{w}}}(\tilde{\boldsymbol{w}}, \boldsymbol{n}) = \begin{bmatrix} -\frac{n_1(\gamma-1)\|\boldsymbol{v}\|^2}{2\rho c^2} & -\frac{n_1(\gamma-1)v_1}{c^2} & -\frac{n_1(\gamma-1)v_2}{c^2} - n_3 & -\frac{n_1(\gamma-1)v_3}{c^2} + n_2 & \frac{n_1(\gamma-1)\|\boldsymbol{v}\|^2}{2\rho c^2} \\ \frac{n_1(\gamma-1)v_1}{\gamma p} & \frac{n_1\rho(\gamma-1)}{\gamma p} & 0 & 0 & -\frac{n_1 v_1 \rho(\gamma-1)}{\gamma p^2} \\ \frac{n_1(\gamma-1)v_2}{\gamma p} & 0 & \frac{n_1\rho(\gamma-1)}{\gamma p} & 0 & -\frac{n_1 v_2 \rho(\gamma-1)}{\gamma p^2} \\ \frac{n_1(\gamma-1)v_3}{\gamma p} & 0 & 0 & \frac{n_1\rho(\gamma-1)}{\gamma p} & -\frac{n_1 v_3 \rho(\gamma-1)}{\gamma p^2} \\ -\frac{n_1\gamma-1}{\rho c^2} & 0 & 0 & 0 & \frac{n_1\gamma-1}{pc^2} \end{bmatrix} \tag{167}$$

$$\frac{\partial l_2}{\partial \tilde{\boldsymbol{w}}}(\tilde{\boldsymbol{w}}, \boldsymbol{n}) = \begin{bmatrix} -\frac{n_2(\gamma-1)\|\boldsymbol{v}\|^2}{2\rho c^2} & -\frac{n_2(\gamma-1)v_1}{c^2} + n_3 & -\frac{n_2(\gamma-1)v_2}{c^2} & -\frac{n_2(\gamma-1)v_3}{c^2} - n_1 & \frac{n_2(\gamma-1)\|\boldsymbol{v}\|^2}{2\rho c^2} \\ \frac{n_2(\gamma-1)v_1}{\gamma p} & \frac{n_2\rho(\gamma-1)}{\gamma p} & 0 & 0 & -\frac{n_2 v_1 \rho(\gamma-1)}{\gamma p^2} \\ \frac{n_2(\gamma-1)v_2}{\gamma p} & 0 & \frac{n_2\rho(\gamma-1)}{\gamma p} & 0 & -\frac{n_2 v_2 \rho(\gamma-1)}{\gamma p^2} \\ \frac{n_2(\gamma-1)v_3}{\gamma p} & 0 & 0 & \frac{n_2\rho(\gamma-1)}{\gamma p} & -\frac{n_2 v_3 \rho(\gamma-1)}{\gamma p^2} \\ -\frac{n_2\gamma-1}{\rho c^2} & 0 & 0 & 0 & \frac{n_2\gamma-1}{pc^2} \end{bmatrix} \tag{168}$$

$$\frac{\partial l_3}{\partial \tilde{\boldsymbol{w}}}(\tilde{\boldsymbol{w}}, \boldsymbol{n}) = \begin{bmatrix} -\frac{n_3(\gamma-1)\|\boldsymbol{v}\|^2}{2\rho c^2} & -\frac{n_3(\gamma-1)v_1}{c^2} - n_2 & -\frac{n_3(\gamma-1)v_2}{c^2} + n_1 & -\frac{n_3(\gamma-1)v_3}{c^2} & \frac{n_3(\gamma-1)\|\boldsymbol{v}\|^2}{2\rho c^2} \\ \frac{n_3(\gamma-1)v_1}{\gamma p} & \frac{n_3\rho(\gamma-1)}{\gamma p} & 0 & 0 & -\frac{n_3 v_1 \rho(\gamma-1)}{\gamma p^2} \\ \frac{n_3(\gamma-1)v_2}{\gamma p} & 0 & \frac{n_2\rho(\gamma-1)}{\gamma p} & 0 & -\frac{n_3 v_2 \rho(\gamma-1)}{\gamma p^2} \\ \frac{n_3(\gamma-1)v_3}{\gamma p} & 0 & 0 & \frac{n_2\rho(\gamma-1)}{\gamma p} & -\frac{n_3 v_3 \rho(\gamma-1)}{\gamma p^2} \\ -\frac{n_3\gamma-1}{\rho c^2} & 0 & 0 & 0 & \frac{n_3\gamma-1}{pc^2} \end{bmatrix} \tag{169}$$

$$\frac{\partial l_4}{\partial \tilde{\boldsymbol{w}}}(\tilde{\boldsymbol{w}}, \boldsymbol{n}) = \begin{bmatrix} \frac{c}{2\rho}\boldsymbol{v}\cdot\boldsymbol{n} & (\gamma-1)v_1 - cn_1 & (\gamma-1)v_2 - cn_2 & (\gamma-1)v_3 - cn_3 & -\frac{c}{2p}\boldsymbol{v}\cdot\boldsymbol{n} \\ -\frac{cn_1}{2\rho} & -(\gamma-1) & 0 & 0 & \frac{cn_1}{2p} \\ -\frac{cn_2}{2\rho} & 0 & -(\gamma-1) & 0 & \frac{cn_2}{2p} \\ -\frac{cn_3}{2\rho} & 0 & 0 & -(\gamma-1) & \frac{cn_3}{2p} \\ 0 & 0 & 0 & 0 & 0 \end{bmatrix} \tag{170}$$

$$\frac{\partial l_5}{\partial \tilde{\boldsymbol{w}}}(\tilde{\boldsymbol{w}}, \boldsymbol{n}) = \begin{bmatrix} \frac{c}{2\rho}\boldsymbol{v}\cdot\boldsymbol{n} & (\gamma-1)v_1 - cn_1 & (\gamma-1)v_2 - cn_2 & (\gamma-1)v_3 - cn_3 & -\frac{c}{2p}\boldsymbol{v}\cdot\boldsymbol{n} \\ \frac{cn_1}{2\rho} & -(\gamma-1) & 0 & 0 & -\frac{cn_1}{2p} \\ \frac{cn_2}{2\rho} & 0 & -(\gamma-1) & 0 & -\frac{cn_2}{2p} \\ \frac{cn_3}{2\rho} & 0 & 0 & -(\gamma-1) & -\frac{cn_3}{2p} \\ 0 & 0 & 0 & 0 & 0 \end{bmatrix} \tag{171}$$

References

[1] Charles R. Doering and J. D. Gibbon. *Applied analysis of the Navier-Stokes equations*. Cambridge University Press, Cambridge, 1995.

[2] C. Farhat, C. Degand, B. Koobus, and M. Lesoinne. Torsional springs for two-dimensional dynamic unstructured fluid meshes. *Computer Methods in Applied Mechanics and Engineering*, 163(1-4):231–245, 1998.

[3] Charbel Farhat, Michel Lesoinne, and Nathan Maman. Mixed explicit/implicit time integration of coupled aeroelastic problems: Three???field formulation, geometric conservation and distributed solution. *International Journal for Numerical Methods in Fluids*, 21(10):807–835, 1995.

[4] J. Frederic Bonnans, J. Charles Gilbert, Claude Lemar??chal, and Claudia A. Sagastiz??bal. Numerical optimization: Theoretical and practical aspects. *Numerical Optimization: Theoretical and Practical Aspects*, pages 1–494, 2006.

[5] Farhat Research Group. Aero-F.

[6] Farhat Research Group. Aero-S.

[7] Michel Lesoinne, Marcus Sarkis, Ulrich Hetmaniuk, and Charbel Farhat. A linearized method for the frequency analysis of three-dimensional uid / structure interaction problems in all ow regimes. 190:1–38, 2001.

[8] Alexander Main. Algorithmic Problems in Social and Geometric Influence a Dissertation Submitted To the Institute for Computational and Mathematical Engineering and the Committee on Graduate Studies of Stanford University in Partial Fulfillment of the Requirements for the. 2014.

[9] K. Maute, M. Nikbay, and C. Farhat. Coupled analytical sensitivity analysis and optimization of three-dimensional nonlinear aeroelastic systems. *AIAA Journal*, 39(11):2051–2061, 2001.

[10] K. Maute, M. Nikbay, and C. Farhat. Sensitivity analysis and design optimization of three-dimensional non-linear aeroelastic systems by the adjoint method. *International Journal for Numerical Methods in Engineering*, 2003.

[11] Serge Piperno and Charbel Farhat. Design of Efficient Partitioned Procedures for the Transient Solution of Aeroelastic Problems. *Revue Européenne des Éléments Finis*, 9(6-7):655–680, jan 2000.

[12] K. Schittkowski, C. Zillober, and R. Zotemantel. Numerical comparison of nonlinear programming algorithms for structural optimization. *Structural Optimization*, 7(1-2):1–19, 1994.

[13] J. A. Sethian. *Level Set Methods and Fast Marching Methods*. Berkeley, 1999.

[14] Jaroslaw Sobieszczanski-Sobieski. Sensitivity of complex, internally coupled systems. *AIAA Journal*, 28(1):153–160, 1990.

[15] Bram van Leer. Towards the ultimate conservative difference scheme. V. A second-order sequel to Godunov's method. *Journal of Computational Physics*, 32(1):101–136, 1979.